Appendix A.38:

Rudds Rd – CPT 5687

Table 1: Site Description for Rudds Rd (CC LIQ 67 – CPT 5687).

Attribute	Yes/No			Description/Date	Symbol in Figure 1
	10-m Buffer	20-m Buffer	50-m Buffer		
Near a body of surface water or other free face features?	No	No	No	The center of the site is ~1200 m to the S from the Avon River (the free-face height is ~2 m) and ~1280 m to the W from the water reserve (the free-face height is ~1.5 m).	NA
Lateral spreading observed during the CES?	No	No	No	No lateral spreading was observed by the mapping team.[1]	NA
Nearby buildings or structures?	Yes	Yes	Yes	Building coverage of the 10-, 20-, and 50-m buffers is 10, 13, and 17%, respectively. Buildings occupy the SE and SW quadrants of the 10- and 20-m buffers and all quadrants of the 50-m buffer.	White Fill + Brown Outline
Sloping land?	No	No	Yes	Residential, predominantly flat area except for the sloping front lawn and driveways at the properties in the N of the 50-m buffer.	NA
Step changes in the ground surface?	No	No	Yes	The properties in the N of the 50-m buffer are ~1 m above the road level.	NA
Retaining walls?	No	No	Yes	Front lawns in the N of the 50-m buffer are retained by ~0.5-m high walls.	NA
Vegetation?	Yes	Yes	Yes	Trees and bushes cover 11, 19, and 32% of the 10-, 20-, and 50-m buffers, respectively. They are in the NW and SW quadrants of the 10-m buffer and all quadrants of the 20- and 50-m buffers.	White Fill + Green Outline
Manmade changes to the site between the LiDAR surveys?	Yes	Yes	Yes	Vegetation and building removal and building addition in the SW q. of the 50-m b. between Mar 2009 and Oct 2009. Addition of two buildings in the SW q. of the 50-m b. between Oct 2009 and Sep 3, 2010. Road construction in the NW q. of the 50-m b. in Oct 2012. Building removal in the SW q. of the 50-m b. between Mar 2014 and Aug 2014. Road construction in all q. of the 50-m b. in Sep 2014. Building removal in the SE and SW q. of all b. between Sep 2014 and Jan 2015. Building addition in all q. of all b. between Jan 2015 and July 2015. Building addition in the NW and SW q. of the 50-m b. between July 2015 and Sep 2015. Building removal in the SW q. of the 20- and 50-m b. between Sep 2015 and Nov 2015.	Building Addition/ Removal: Orange Outline/ Crossline; Vegetation Removal: Green Crossline
Other important factors?	No	Yes	Yes	Low-motor-vehicle-volume, two-way roadway (street) occupies 17% and 13% of the 20-m and 50-m buffers, respectively, and runs in the E-W direction through the NE and NW quadrants of the 20-m and 50-m buffers.	Road: Gray Fill + Red Outline

Note: Buffer is the area within a circle of a specified radius with CPT investigations done at its center (172.686716°, -43.527755°).

[1] Canterbury Geotechnical Database. (2012). "Observed Ground Crack Locations", Map Layer CGD0400 - 23 July 2012, retrieved July 09, 2018 from https://canterburygeotechnicaldatabase.projectorbit.com/

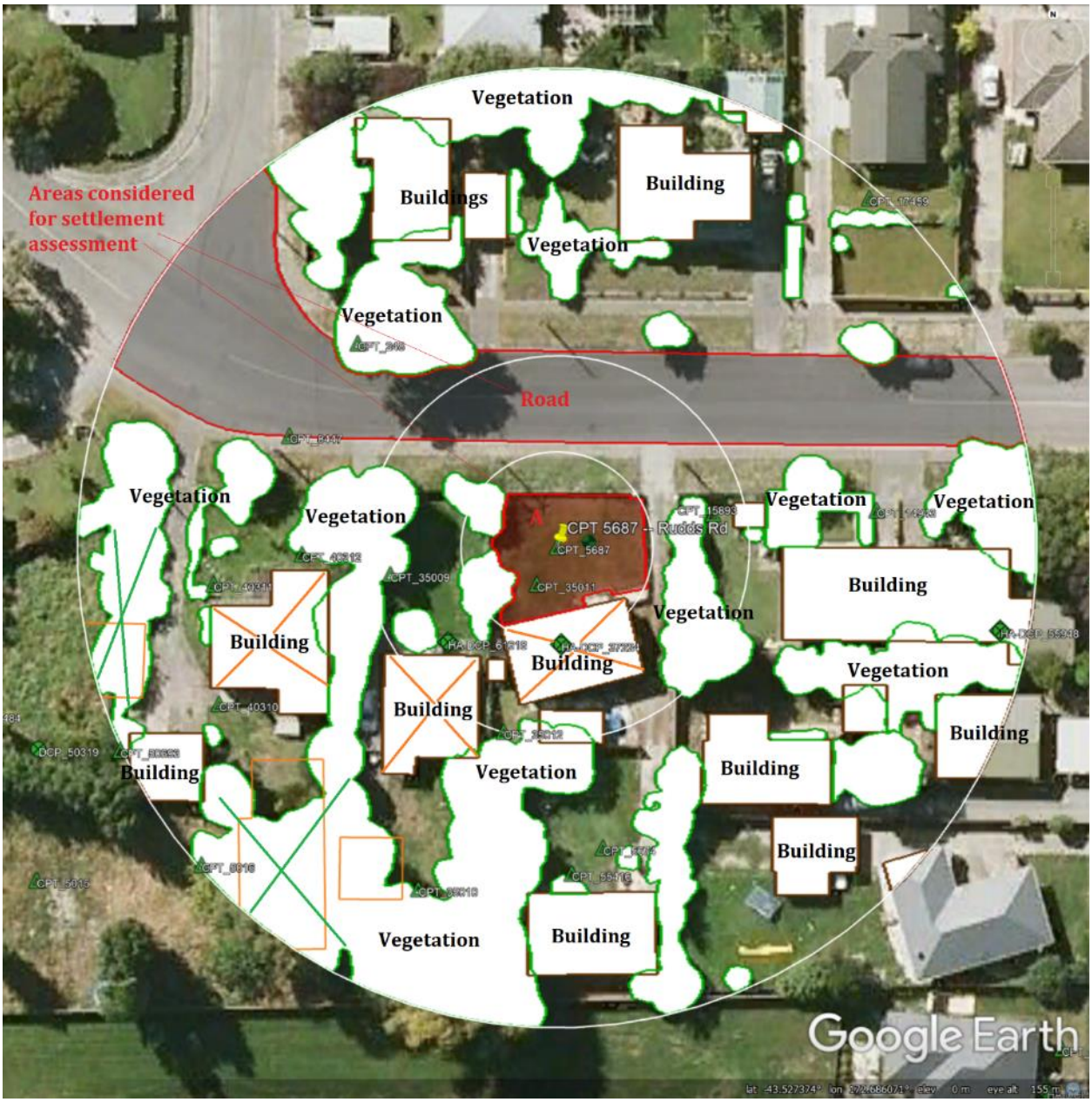

Figure 1: Site plan with areas where ejecta-induced settlement is considered.

Note 1: Patch A (outlined in red) in the free field was selected for settlement assessment as an area free of vegetation and structures. Other important factors considered in the patch selection process were its proximity to a CPT, a property subjected to addition and/or demolition of a structure, front yard/backyard alterations (e.g., ploughing, rubble, scrap), and aerial distribution of sediment ejecta. In addition, the entire portion of the road within the 50-m buffer was considered for settlement assessment. The LiDAR-based settlement analyses for Patch A were not performed for any EQ event due to the evident absence of ejecta for the Sep-10 and Dec-11 EQs and uncertainties explained in Table 2 for the Feb-11 and Jun-11 EQs. The LiDAR-based settlement analyses for Road were not performed because ejecta were not observed for the Sep-10 and Dec-11 EQs and only negligible ejecta were observed for the Feb-11 and Jun-11 EQs.

Table 2: LiDAR flight error adjustments, global adjustments for the difference between average LiDAR point elevations and benchmark survey elevations, and vertical tectonic movement adjustments.

	Adjustments (mm)		
Earthquake Event(s)	LiDAR Flight Error	Global Offset[2]	Tectonic Vertical Movement
Sep-10	0	-3	0
Feb-11	0	16	+165
Jun-11	0	38	-50
Dec-11	0	-65	+20
CES	0	-14	+135
Any LiDAR survey affected by ejecta?			Yes*

Notes: The negative sign indicates the subtraction from the ground surface subsidence, while the positive sign indicates the addition to the ground surface subsidence; Ejecta from the Feb-11 EQ might have remained within Patch A through Nov 2011 thus affecting the LiDAR survey measurements for the Feb-11, Jun-11, and Dec-11 EQs; Significant tectonic vertical movement (uplift) is estimated for the Feb-11 EQ.

Table 3a: LiDAR Measurement Error for Patch A.

Surveys	Buffer	Area Averaged Difference Indicating Repeat Measurement Error (mm)	$\sigma^*_{\text{individual LiDAR points}}$ (mm)	%Reduction in σ due to Area Averaging of LiDAR Points
Post Feb 2011: Mar 2011 and May 2011	10-m	ND	59	[ND,ND]
	20-m	ND		
	50-m	ND		
Post Dec 2011: Feb 2012 and Oct 2015	10-m	ND	70	[ND,ND]
	20-m	ND		
	50-m	ND		

*Standard deviation; ND = Not determined.

[2] Russell, J., & van Ballegooy, S. (2015). *Canterbury Earthquake Sequence: Increased liquefaction vulnerability assessment methodology*. New Zealand: Tonkin & Taylor Ltd.

Table 3b: LiDAR Measurement Error for Road.

Surveys	Buffer	Area Averaged Difference Indicating Repeat Measurement Error (mm)	$\sigma^*_{\text{individual LiDAR points}}$ (mm)	%Reduction in σ due to Area Averaging of LiDAR Points
Post Feb 2011: Mar 2011 and May 2011	10-m	NA	59	[ND,ND]
	20-m	ND		
	50-m	ND		
Post Dec 2011: Feb 2012 and Oct 2015	10-m	NA	70	[ND,ND]
	20-m	ND		
	50-m	ND		

*Standard deviation; NA = Not available; ND = Not determined.

Table 4a: Ground surface subsidence adjustments due to LiDAR measurement error for Patch A.

Earthquake Event(s)	$\sigma_{\text{pre-EQ LiDAR survey}}$ (mm)	$\sigma_{\text{post-EQ LiDAR survey}}$ (mm)	σ_{total} (mm)	Area Average Adjusted σ (mm) **
Sep-10	158	56	134	ND
Feb-11	56	59	59	ND
Jun-11	59	61	62	ND
Dec-11	61	70	87	ND
CES	158	70	124	ND

**Based on the highest %Reduction in Table 3a.

Table 4b: Ground surface subsidence adjustments due to LiDAR measurement error for Road.

Earthquake Event(s)	$\sigma_{\text{pre-EQ LiDAR survey}}$ (mm)	$\sigma_{\text{post-EQ LiDAR survey}}$ (mm)	σ_{total} (mm)	Area Average Adjusted σ (mm) **
Sep-10	158	56	134	ND
Feb-11	56	59	59	ND
Jun-11	59	61	62	ND
Dec-11	61	70	87	ND
CES	158	70	124	ND

**Based on the highest %Reduction in Table 3b.

Table 5a: Raw liquefaction-related ground surface subsidence using original LiDAR points for Patch A.

	Average Ground Surface Subsidence (mm)		
Earthquake Event(s)	10-m Buffer	20-m Buffer	50-m Buffer
Sep-10	ND	ND	ND
Feb-11	ND	ND	ND
Jun-11	ND	ND	ND
Dec-11	ND	ND	ND
CES	ND	ND	ND

Table 5b: Raw liquefaction-related ground surface subsidence using original LiDAR points for Road.

	Average Ground Surface Subsidence (mm)		
Earthquake Event(s)	10-m Buffer	20-m Buffer	50-m Buffer
Sep-10	NA	ND	ND
Feb-11	NA	ND	ND
Jun-11	NA	ND	ND
Dec-11	NA	ND	ND
CES	NA	ND	ND

Table 6a: Corrected liquefaction-related ground surface subsidence using original LiDAR points for Patch A with the calculated adjustments in Table 2.

	Average Calculated Ground Surface Subsidence (mm)		
Earthquake Event(s)	10-m Buffer	20-m Buffer	50-m Buffer
Sep-10	ND	ND	ND
Feb-11	ND	ND	ND
Jun-11	ND	ND	ND
Dec-11	ND	ND	ND
CES	ND	ND	ND

Notes: Plus/minus values are same as those in Table 4a, but rounded to the nearest 25 mm; Positive overall values indicate ground surface subsidence, while negative overall values indicate ground surface uplift; ND = Not determined.

Table 6b: Corrected liquefaction-related ground surface subsidence using original LiDAR points for Road with the calculated adjustments in Table 2.

	Average Calculated Ground Surface Subsidence (mm)		
Earthquake Event(s)	10-m Buffer	20-m Buffer	50-m Buffer
Sep-10	NA	ND	ND
Feb-11	NA	ND	ND
Jun-11	NA	ND	ND
Dec-11	NA	ND	ND
CES	NA	ND	ND

Notes: Plus/minus values are same as those in Table 4b, but rounded to the nearest 25 mm; Positive overall values indicate ground surface subsidence, while negative overall values indicate ground surface uplift; NA = Not available; ND = Not determined.

Table 7a: Corrected liquefaction-related ground surface subsidence for Patch A using LiDAR DEMs.

	Estimated Ground Surface Subsidence (mm)								
	10-m Buffer			20-m Buffer			50-m Buffer		
Earthquake Event(s)	16^{th} %ile	50^{th} %ile	84^{th} %ile	16^{th} %ile	50^{th} %ile	84^{th} %ile	16^{th} %ile	50^{th} %ile	84^{th} %ile
Sep-10	<50	<50	<50	<50	<50	<50	<50	<50	<50
Feb-11	250	250	350	250	250	350	250	250	350
Jun-11	<50	50	50	<50	50	50	<50	50	50
Dec-11	<50	<50	<50	<50	<50	<50	<50	<50	<50
CES	250	350	450	250	350	450	250	350	450

Note: These percentiles are not the exact statistical measures; they indicate the spatial variability of ground surface subsidence.

Table 7b: Corrected liquefaction-related ground surface subsidence for Road using LiDAR DEMs.

	Estimated Ground Surface Subsidence (mm)								
	10-m Buffer			20-m Buffer			50-m Buffer		
Earthquake Event(s)	16^{th} %ile	50^{th} %ile	84^{th} %ile	16^{th} %ile	50^{th} %ile	84^{th} %ile	16^{th} %ile	50^{th} %ile	84^{th} %ile
Sep-10	NA	NA	NA	<50	<50	<50	<50	<50	<50
Feb-11	NA	NA	NA	150	200	250	200	250	300
Jun-11	NA	NA	NA	<50	50	50	<50	50	100
Dec-11	NA	NA	NA	<50	<50	<50	<50	<50	<50
CES	NA	NA	NA	250	350	350	250	350	500

Note: These percentiles are not the exact statistical measures; they indicate the spatial variability of ground surface subsidence.

Table 8a: Ejecta-Induced settlement for the top 20 m of the soil profile for Patch A for the 50th %ile PGA, P_L=50%, and C_{FC}=0.13 using BI-2014, ZRB-2002, and I_C cutoff of 2.6.

Earthquake Event(s)	M_W	PGA (g)	Depth to Groundwater (m)	S_T (mm)	S_{V1D} (mm)	$S_{E,L}$ (mm)
Sep-10	7.1	0.21	0.5-1.5	ND	33±20	ND
Feb-11	6.2	0.63	0.7-1.7	ND	94±50	ND
Jun-11	6.2	0.36	1.0-2.0	ND	45±25	ND
Dec-11	6.1	0.29	1.5-2.5	ND	25±50	ND

Notes: S_T = Total settlement (Table 6); S_{V1D} = Average vertical settlement due to volumetric compression using Boulanger and Idriss (2014) (BI-2014), Zhang et al. (2002) (ZRB-2002) procedures and de Greef and Lengkeek (2018) thin-layer correction; $S_{E,L}$ = Ejecta-induced settlement as the difference between the LiDAR-based S_T and S_{V1D}; The groundwater depth is provided as a range due to the difference in ground surface elevation (the northern portion of the 50-m buffer is ~1 m above the rest of the site).

Table 8b: Ejecta-Induced settlement for the top 20 m of the soil profile for Road (20-m buffer) for the 50th %ile PGA, P_L=50%, and C_{FC}=0.13 using BI-2014, ZRB-2002, and I_C cutoff of 2.6.

Earthquake Event(s)	M_W	PGA (g)	Depth to Groundwater (m)	S_T (mm)	S_{V1D} (mm)	$S_{E,L}$ (mm)
Sep-10	7.1	0.21	0.5-1.5	ND	28±20	ND
Feb-11	6.2	0.63	0.7-1.7	ND	101±50	ND
Jun-11	6.2	0.36	1.0-2.0	ND	42±25	ND
Dec-11	6.1	0.29	1.5-2.5	ND	21±50	ND

Notes: S_T = Total settlement (Table 6); S_{V1D} = Average vertical settlement due to volumetric compression using Boulanger and Idriss (2014) (BI-2014), Zhang et al. (2002) (ZRB-2002) procedures and de Greef and Lengkeek (2018) thin-layer correction; $S_{E,L}$ = Ejecta-induced settlement as the difference between the LiDAR-based S_T and $S_{V1D;}$ The groundwater depth is provided as a range due to the difference in ground surface elevation (the northern portion of the 50-m buffer is ~1 m above the rest of the site).

Table 8c: Ejecta-Induced settlement for the top 20 m of the soil profile for Road (50-m buffer) for the 50th %ile PGA, P_L=50%, and C_{FC}=0.13 using BI-2014, ZRB-2002, and I_C cutoff of 2.6.

Earthquake Event(s)	M_W	PGA (g)	Depth to Groundwater (m)	S_T (mm)	S_{V1D} (mm)	$S_{E,L}$ (mm)
Sep-10	7.1	0.21	0.5-1.5	ND	28±20	ND
Feb-11	6.2	0.63	0.7-1.7	ND	107±50	ND
Jun-11	6.2	0.36	1.0-2.0	ND	46±25	ND
Dec-11	6.1	0.29	1.5-2.5	ND	21±50	ND

Notes: S_T = Total settlement (Table 6); S_{V1D} = Average vertical settlement due to volumetric compression using Boulanger and Idriss (2014) (BI-2014), Zhang et al. (2002) (ZRB-2002) procedures and de Greef and Lengkeek (2018) thin-layer correction; $S_{E,L}$ = Ejecta-induced settlement as the difference between the LiDAR-based S_T and S_{V1D}; The groundwater depth is provided as a range due to the difference in ground surface elevation (the northern portion of the 50-m buffer is ~1 m above the rest of the site).

Note 2: The uncertainty for volumetric settlement was derived based on the sensitivity of volumetric settlement to PGA, C_{FC}, and P_L for each earthquake event for VsVp 57203 *Shirley Intermediate School* and CC LIQ 1 – CPT 5586 – *Vivian St* sites. Taking the 50th percentile as the baseline case, the minimum and maximum values corresponding to the difference between the 25th percentile and the 50th percentile and the 75th percentile and the 50th percentile were determined. The arithmetic mean of the range of the minimum and maximum difference was evaluated for each patch at the two sites. The maximum arithmetic mean for each earthquake event was rounded to the nearest five and used as the uncertainty value. Accordingly, the 1-D volumetric settlement uncertainties of ±20, ±50, ±25, and ±50 mm for the Sep-10, Feb-11, Jun-11, and Dec-11 earthquake events, respectively, were used for all sites in this study.

Table 9a: Coverage area and height of ejecta estimates for Patch A using photographs.

Earthquake Event	$A_{E,thick1}$ (m^2)	$H_{E,thick1}$ (mm)	$A_{E,thick2}$ (m^2)	$H_{E,thick2}$ (mm)	$A_{E,thin1}$ (m^2)	$H_{E,thin1}$ (mm)	$A_{E,thin2}$ (m^2)	$H_{E,thin2}$ (mm)	A_T (m^2)
Sep-10	0	0	0	0	0	0	0	0	168
Feb-11	22.7	100-160	20.9	40-80	7.6	30-70	46.7	20-30	160*
Jun-11	7.5	60-120	0	0	34.5**	30-50**	0	0	164
Dec-11	0	0	0	0	0	0	0	0	168

Notes: $A_{E,thick/thin}$ = Coverage area of thick/thin ejecta layers; $H_{E,thick/thin}$ = Lower-upper estimate of height of thick/thin ejecta layers; A_T = Total assessment area of a buffer being considered; Thin and thick layers correspond to light gray and dark gray colors of ejecta observed in aerial photographs; * indicates reduction in A_T due to the presence of objects; ** Ejecta might be a result of the Feb-11 EQ.

Table 9b: Coverage area and height of ejecta estimates for Road (20-m buffer) using photographs.

EQ Event	$H_{E,thin}$ (mm)	$A_{E,thin}$ (m^2)	$H_{E,prism/pyr}$ (mm)	$V_{E,prism+pyr}$ (m^3)	A_T (m^2)
Sep-10	0	0	0	0	226
Feb-11	2-4	17.3	0	0	226
Jun-11	2-4	99.7	0	0	210*
Dec-11	0	0	0	0	226

Notes: $A_{E,thin}$ = Coverage area of thin ejecta layers; $H_{E,\ thin}$ = Lower-upper estimate of height of thin ejecta layers; $H_{E,prism/pyr}$ = Lower-upper estimate of ejecta height near the curb based on 2-4% cross slope of normal crown; $V_{E,prism/pyr}$ = Lower-upper estimate of total volume of prismatic-shape ejecta; $V_{E,prism/pyr}$ = Lower-upper estimate of total volume of prismatic-shape and pyramidal-shape ejecta; A_T= Total assessment area of a buffer being considered; * indicates reduction in A_T due to the presence of objects/shadows.

Table 9c: Coverage area and height of ejecta estimates for Road (50-m buffer) using photographs.

EQ Event	$H_{E,thin}$ (mm)	$A_{E,thin}$ (m^2)	$H_{E,thick}$ (mm)	$V_{E,thick}$ (m^3)	$H_{E,prism/pyr}$ (mm)	$V_{E,prism+pyr}$ (m^3)	A_T (m^2)
Sep-10	0	0	0	0	0	0	1052
Feb-11	2-4	63.4	5-10	16.7	15-64	0.21-0.41	1052
Jun-11	2-4	270	0	0	0	0	952*
Dec-11	0	0	0	0	0	0	1052

Notes: $A_{E,thin/thick}$ = Coverage area of thin/thick ejecta layers; $H_{E,\ thin}$ = Lower-upper estimate of height of thin/thick ejecta layers; $H_{E,prism/pyr}$ = Lower-upper estimate of ejecta height near the curb based on 2-4% cross slope of normal crown; $V_{E,prism/pyr}$ = Lower-upper estimate of total volume of prismatic-shape ejecta; $V_{E,prism/pyr}$ = Lower-upper estimate of total volume of prismatic-shape and pyramidal-shape ejecta; A_T= Total assessment area of a buffer being considered; * indicates reduction in A_T due to the presence of objects/shadows.

Note 3: The values in Table 9 correspond to the coverage area of ejecta outlined in aerial photographs (Figures 26, 28, 30, 46, and 47) and the lower and upper estimates of ejecta height based on geometrical approximations, ground photographs (Figure 48), and EQC LDAT property inspection reports (Figure 49). The ejecta-induced settlement using photographs and engineering judgment, $S_{E,P}$, is estimated as

$$S_{E,P} = \frac{\sum_{i=1}^{a} A_{E,thick,i} * H_{E,thick,i} + \sum_{j=1}^{b} A_{E,thin,j} * H_{E,thin,j}}{A_T} + \frac{\frac{1}{2}\sum_{n=1}^{f} W_{E,prism,n} * H_{E,prism,n} * L_{E,prism,n} + \frac{1}{6}\sum_{p=1}^{g} W_{E,pyramid,p} * H_{E,pyramid} * L_{E,pyramid}}{A_T} = \frac{\sum_{i=1}^{a} V_{E,thick,i} + \sum_{j=1}^{b} V_{E,thin,j} + \sum_{n=1}^{f} V_{E,prism,n} + \sum_{p=1}^{g} V_{E,pyramid,p}}{A_T}$$

where

- $A_{E,thick,i}$ and $H_{E,thick,i}$ are the area and the height of a thick ejecta layer, respectively;

- $A_{E,thin,j}$ and $H_{E,thin,j}$ are the area and the height of a thin ejecta layer, respectively;
- $W_{E,prism,n}$ and $L_{E,prism,n}$ are the width and the length of the coverage area of a prismatically shaped ejecta layer, respectively, and $H_{E,prism,n}$ is the height of a prism-like ejecta layer;
- $W_{E,pyr,p}$ and $L_{E,pyr,p}$ are the width and the length, respectively, of the coverage area of a an ejecta layer shaped a triangular pyramid, and $H_{E,pyr,p}$ is the height of the pyramid-like ejecta layer;
- A_T is the total assessment area for a buffer being considered (Figure 1).

Table 10: Ejecta-induced settlement estimates for Patch A and Road based on photographs.

Earthquake Event	Patch A (10-, 20-, and 50-m buffers)		Road (20-m buffer)		Road (50-m buffer)	
	$S_{E,P,lower}$ (mm)	$S_{E,P,upper}$ (mm)	$S_{E,P,lower}$ (mm)	$S_{E,P,upper}$ (mm)	$S_{E,P,lower}$ (mm)	$S_{E,P,upper}$ (mm)
Sep-10	0	0	0	0	0	0
Feb-11	27	45	≈0	≈0	≈0	1
Jun-11	9	16	1	2	≈0	1
Dec-11	0	0	0	0	0	0

Note: $S_{E,P,lower}$ and $S_{E,P,upper}$ correspond to lower and upper estimates of $S_{E,P}$, respectively.

Table 11: Best final estimates of ejecta-induced settlement for Patch A and Road.

EQ Event	Patch A (10-, 20-, and 50-m buffers)			Road (20-m buffer)			Road (50-m buffer)		
	$S_{E,L}$ (mm)	$S_{E,P}$ (mm)	$S_{E,final}$ (mm)	$S_{E,L}$ (mm)	$S_{E,P}$ (mm)	$S_{E,final}$ (mm)	$S_{E,L}$ (mm)	$S_{E,P}$ (mm)	$S_{E,final}$ (mm)
Sep-10	ND	0	0	ND	0	0	ND	0	0
Feb-11	ND	36±9	35±10	ND	≈0	<5	ND	0.5±0.5	<5
Jun-11	ND	13±3	15±5	ND	1.5±0.5	<5	ND	0.5±0.5	<5
Dec-11	ND	0	0	ND	0	0	ND	0	0

Notes: $S_{E,L}$ = Ejecta-induced settlement based on LiDAR data reported in Table 8; $S_{E,P}$ = Median ejecta-induced settlement for the range of values reported in Table 10; $S_{E,final}$ = Best final estimate of ejecta-induced settlement rounded to the nearest 5; Final plus/minus values are also rounded to the nearest 5 mm; ND = Not determined.

Note 4:

- $S_{E,final}$ for Patch A and Road is based solely on $S_{E,P}$ for all earthquake events due to the evident absence of ejecta or uncertainties explained in Table 2.
- The Rudds Rd site is not in the apparent zone of higher/lower ground surface subsidence for the Sep-10 or Feb-11 EQ, but in the zone of large vertical tectonic movement (uplift) for the Feb-11 EQ. The site is in the zone of accurate LPI prediction of liquefaction severity for the Sep-10 EQ and slight LPI overprediction of liquefaction severity for the Feb-11 EQ (Maurer

et al. 2014[3]). The LDAT property inspection report and ground photographs are available for Patch A. The ejecta height of 300 mm at one of the properties within the 50-m buffer was recorded at the time of the inspection (Nov 2011). There are no ground photographs of the road.

Summary 1:

- **The best estimate of the ejecta-induced free-field ground settlement at the Rudds Rd site for the SEP 2010, FEB 2011, JUN 2011, and DEC 2011 earthquake is 0 mm, 35±10 mm, 15±5 mm, and 0 mm, respectively.**
- **The best estimate of the ejecta-induced free-field ground settlement of the road at the Rudds Rd site for the SEP 2010, FEB 2011, JUN 2011, and DEC 2011 earthquake is 0 mm, <5 mm, <5 mm, and 0 mm, respectively.**

Figure 2: Location of the site.

[3] Maurer, B. W., Green, R. A., Cubrinovski, M., & Bradley, B. A. (2014). Evaluation of the Liquefaction Potential Index for Assessing Liquefaction Hazard in Christchurch, New Zealand. *Journal of Geotechnical and Geoenvironmental Engineering*, 140(7), 04014032-1-11. doi:10.1061/(asce)gt.1943-5606.0001117

Figure 3: Position of the site relative to nearby free-face features.

Figure 4: Position of the site relative to nearby buildings and vegetation.

Figure 5: Street view of the flat land (the S half of the 50-m buffer).

Figure 6: Street view of the sloping land (the N half of the 50-m buffer).

Figure 7: Satellite image of the site taken in Dec 2004.

Figure 8: Satellite image of the site taken in Mar 2009.

Figure 9: Satellite image of the site taken in Oct 2009.

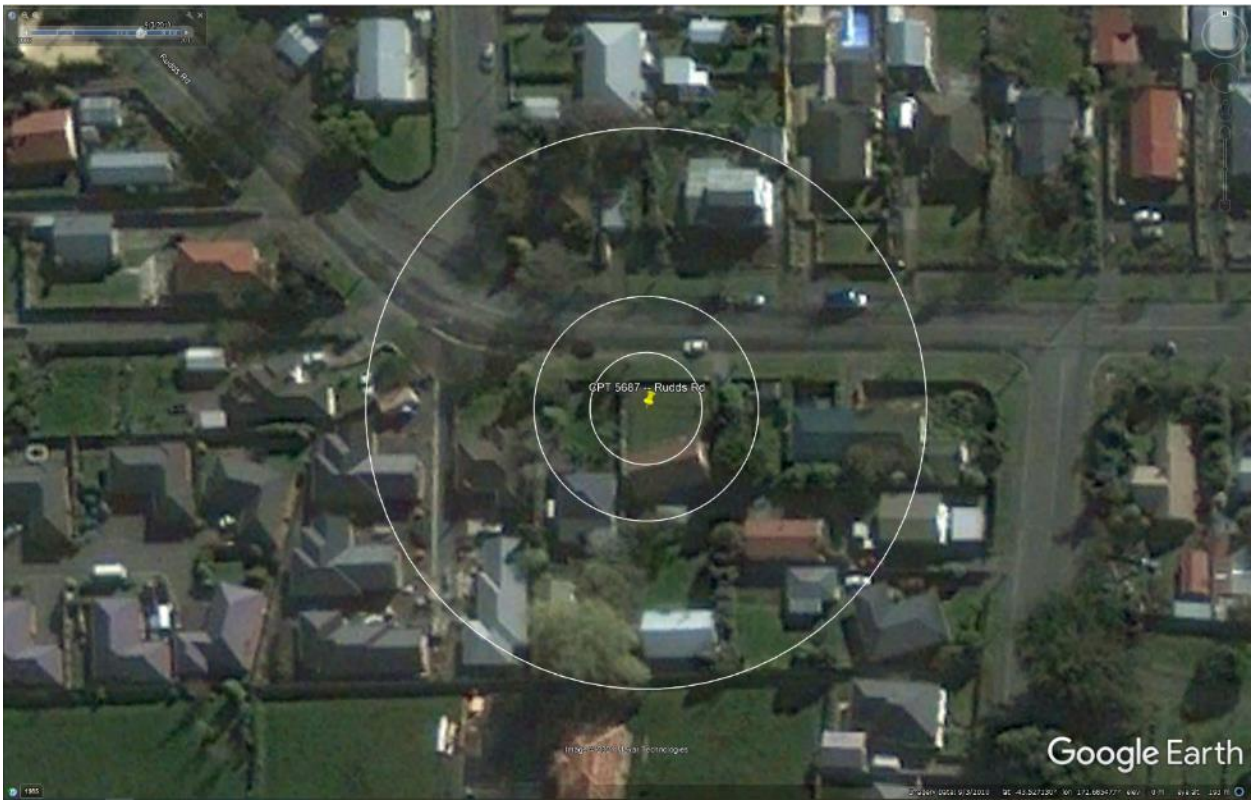

Figure 10: Satellite image of the site taken on Sep 3, 2010.

Figure 11: Satellite image of the site taken on Sep 5, 2010.

Figure 12: Satellite image of the site taken on Feb 7, 2011.

Figure 13: Satellite image of the site taken on Feb 15, 2011.

Figure 14: Satellite image of the site taken on Feb 23, 2011.

Figure 15: Satellite image of the site taken on Feb 26, 2011.

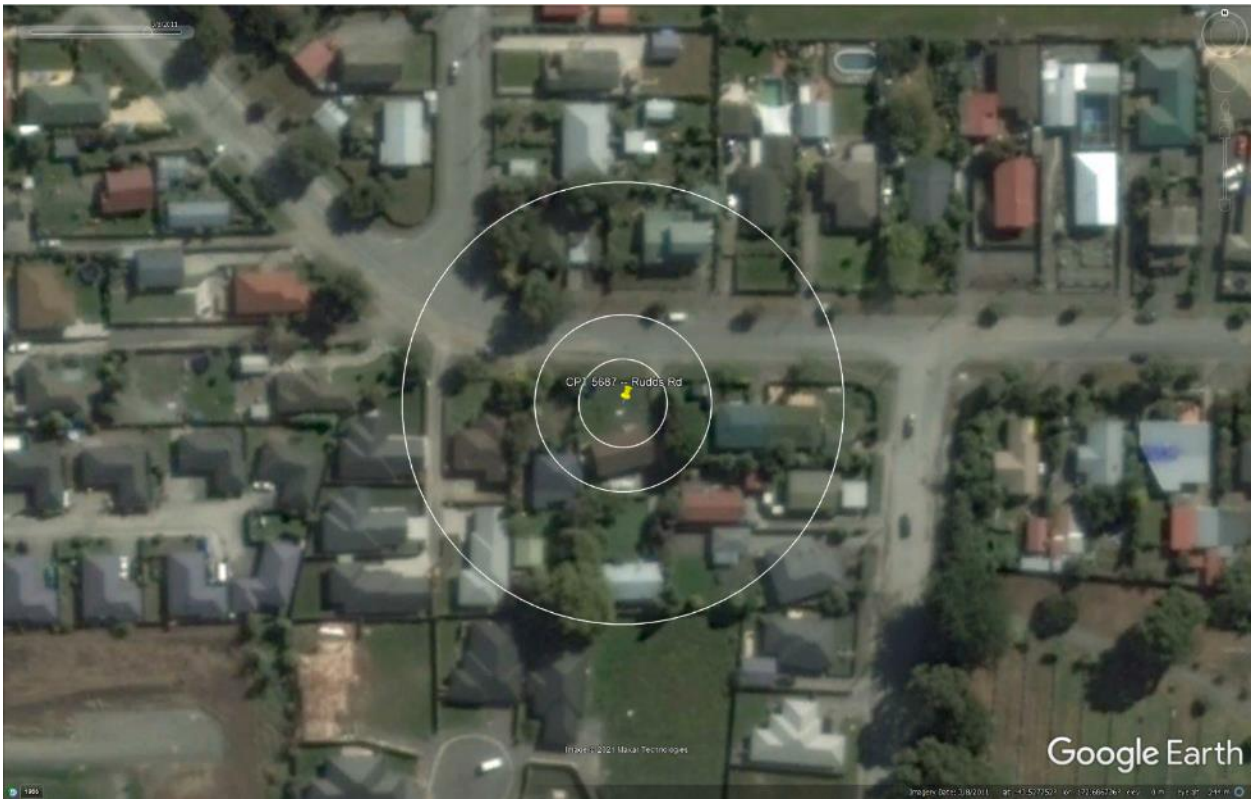

Figure 16: Satellite image of the site taken on Mar 8, 2011.

Figure 17: Satellite image of the site taken in Apr 2012.

Figure 18 Satellite image of the site taken in Oct 2012.

Figure 19: Satellite image of the site taken in Mar 2014.

Figure 20: Satellite image of the site taken in Aug 2014.

Figure 21: Satellite image of the site taken in Sep 2014.

Figure 22: Satellite image of the site taken in Jan 2015.

Figure 23: Satellite image of the site taken in Jul 2015.

Figure 24: Satellite image of the site taken in Sep 2015.

Figure 25: Satellite image of the site taken in Nov 2015.

Figure 26: Aerial photograph of the site taken on Sep 4, 2010 (what appears to be a thin layer of ejecta on the road in the NW quadrant of the 50-m buffer is more likely soil that remained on the road after the building and driveway construction in the E portion of the 50-m buffer).

Figure 27: Aerial photograph of the site taken on Feb 24, 2011.

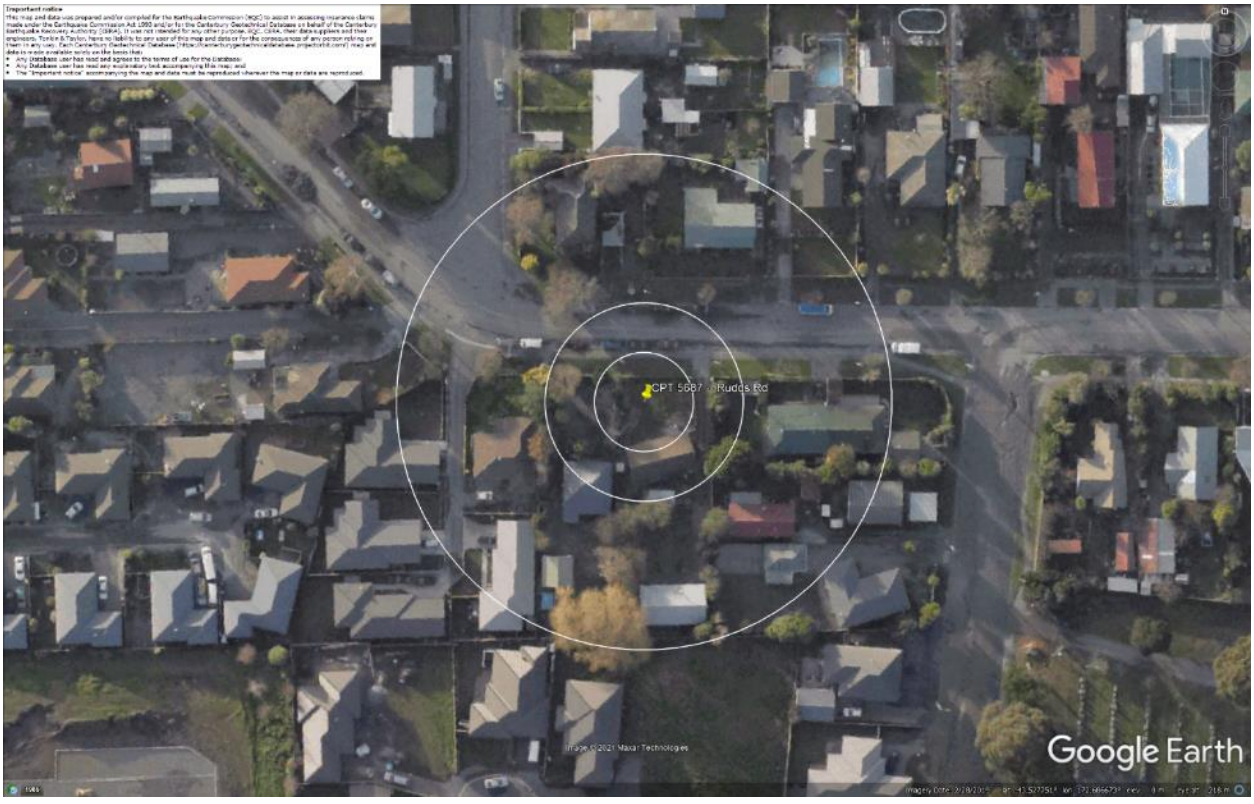

Figure 28: Aerial photograph of the site taken on June 14-15, 2011.

Figure 29: Aerial photograph of the site taken on June 16, 2011.

Figure 30: Aerial photograph of the site taken on Dec 24, 2011.

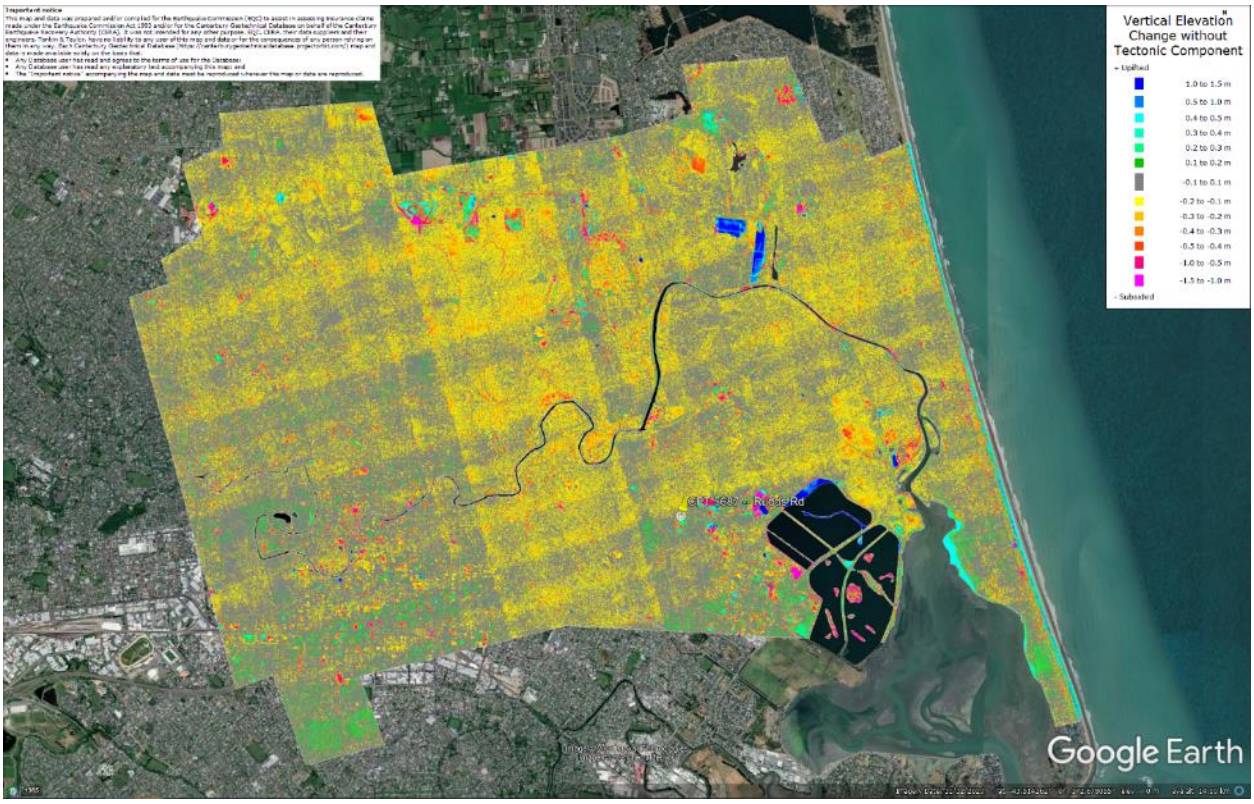

Figure 31: Vertical Ground Movements (Surface – Tectonic) for Sep 2010 Earthquake – the site is not in the apparent zone of overestimated ground surface subsidence.

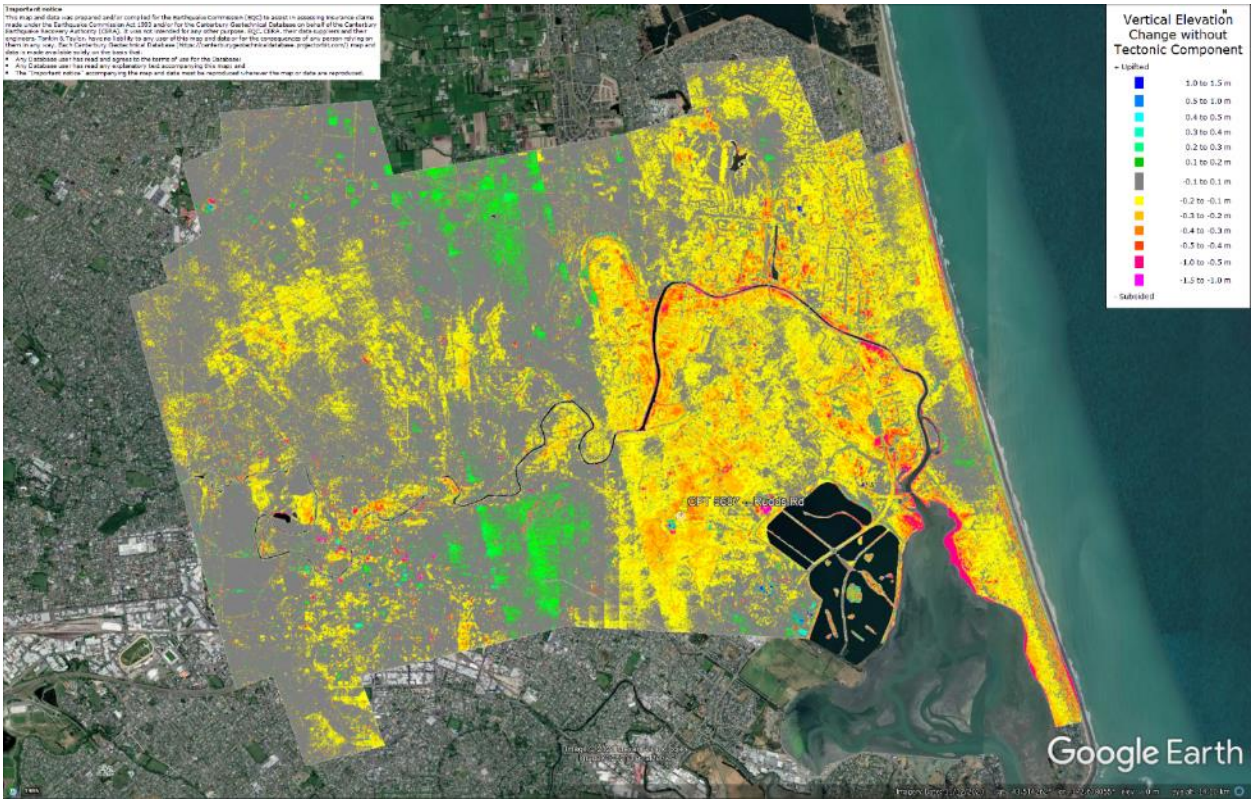

Figure 32: Vertical Ground Movements (Surface – Tectonic) for Feb 2011 Earthquake – the site is not in the apparent zone of underestimated ground surface subsidence.

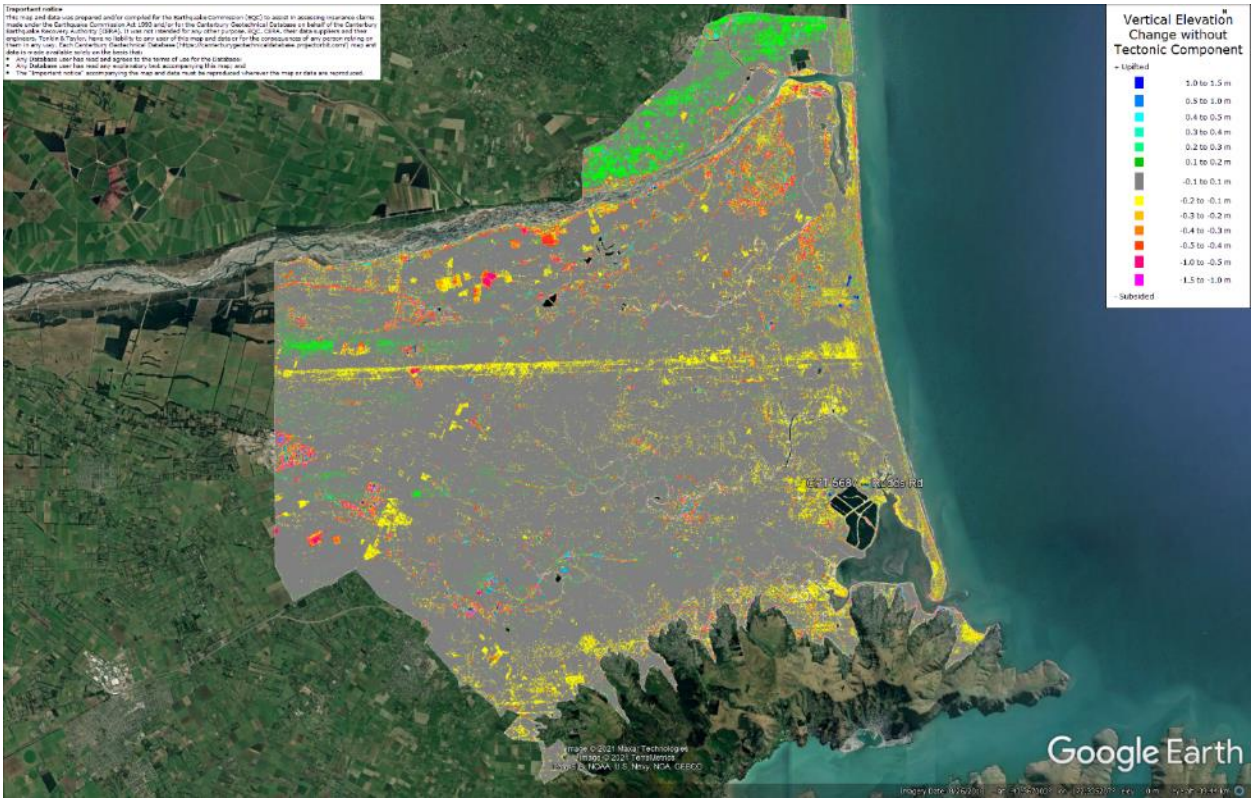

Figure 33: Vertical Ground Movements (Surface – Tectonic) for June 2011 Earthquake – the site is not in the apparent zone of overestimated or underestimated ground surface subsidence.

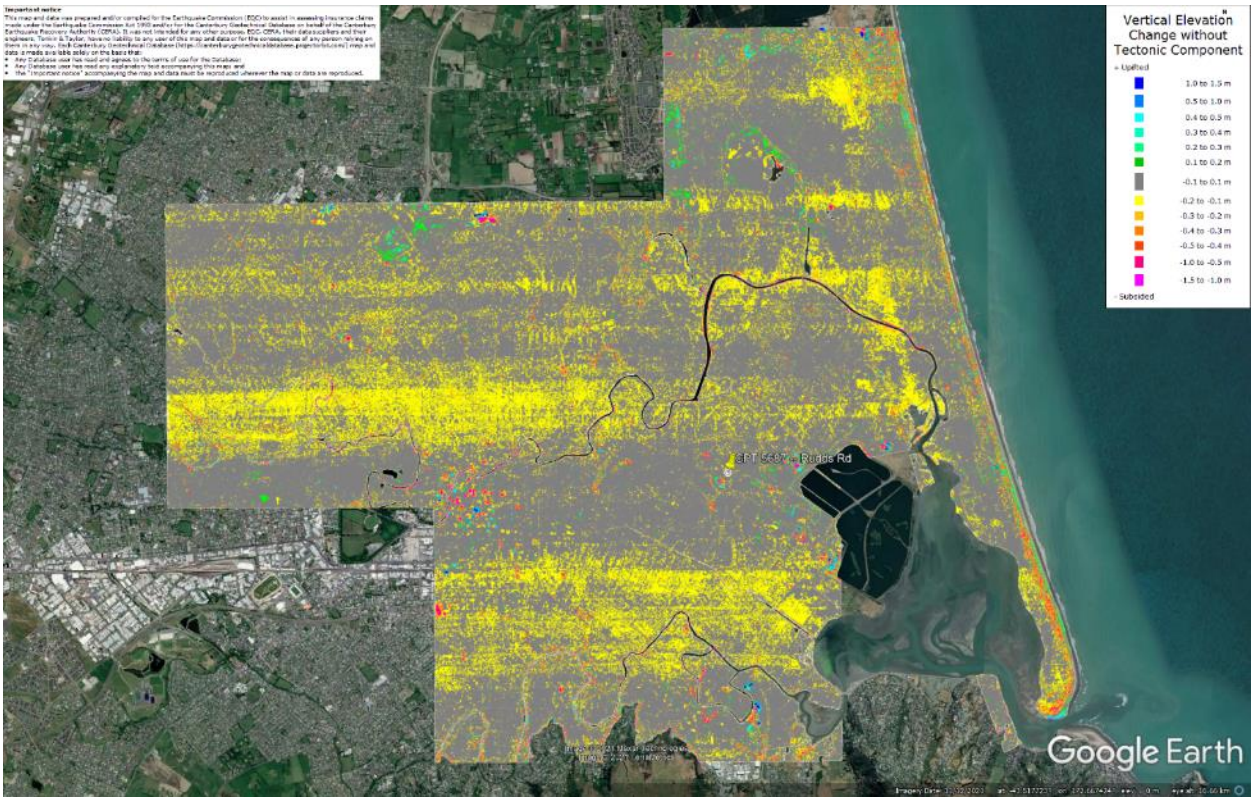

Figure 34: Vertical Ground Movements (Surface – Tectonic) for Dec 2011 Earthquake – the site is not in the apparent zone of overestimated or underestimated ground surface subsidence.

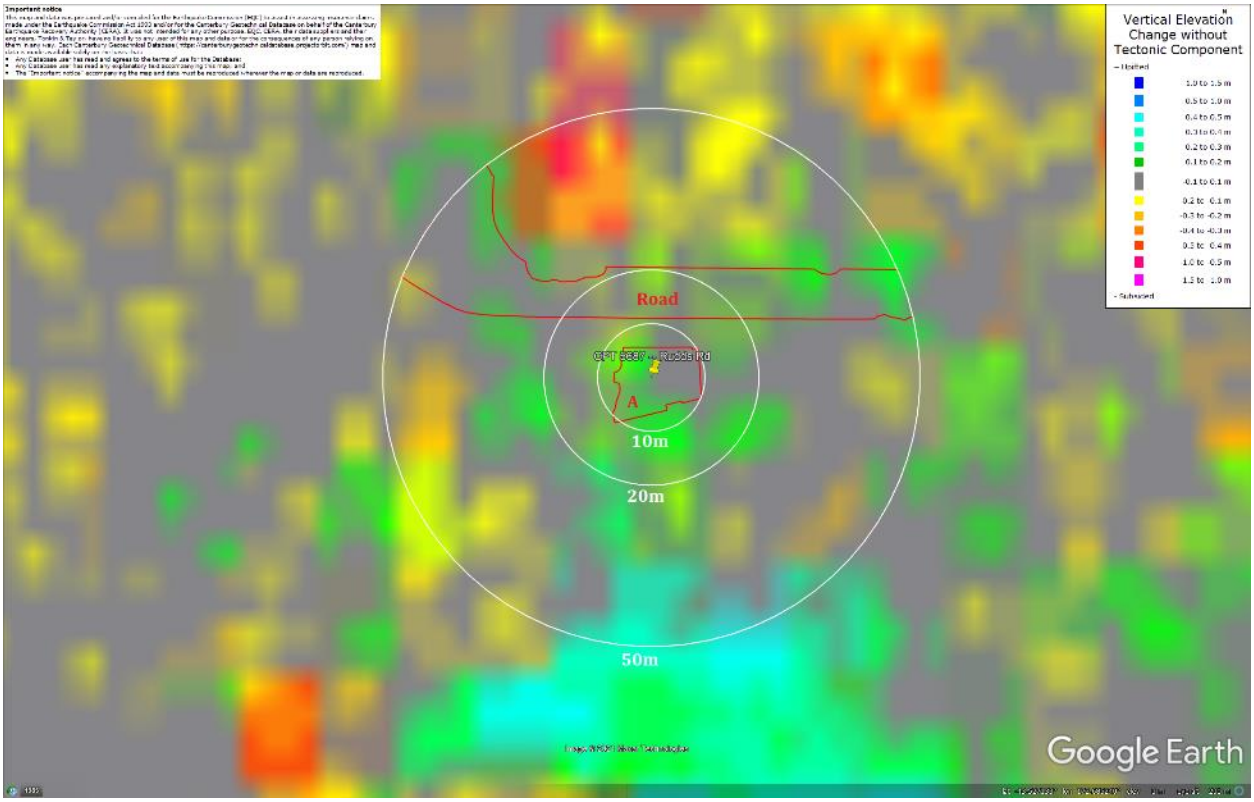

Figure 35: Ground surface subsidence without tectonic component for Sep 2010 Earthquake according to the LiDAR DEM.

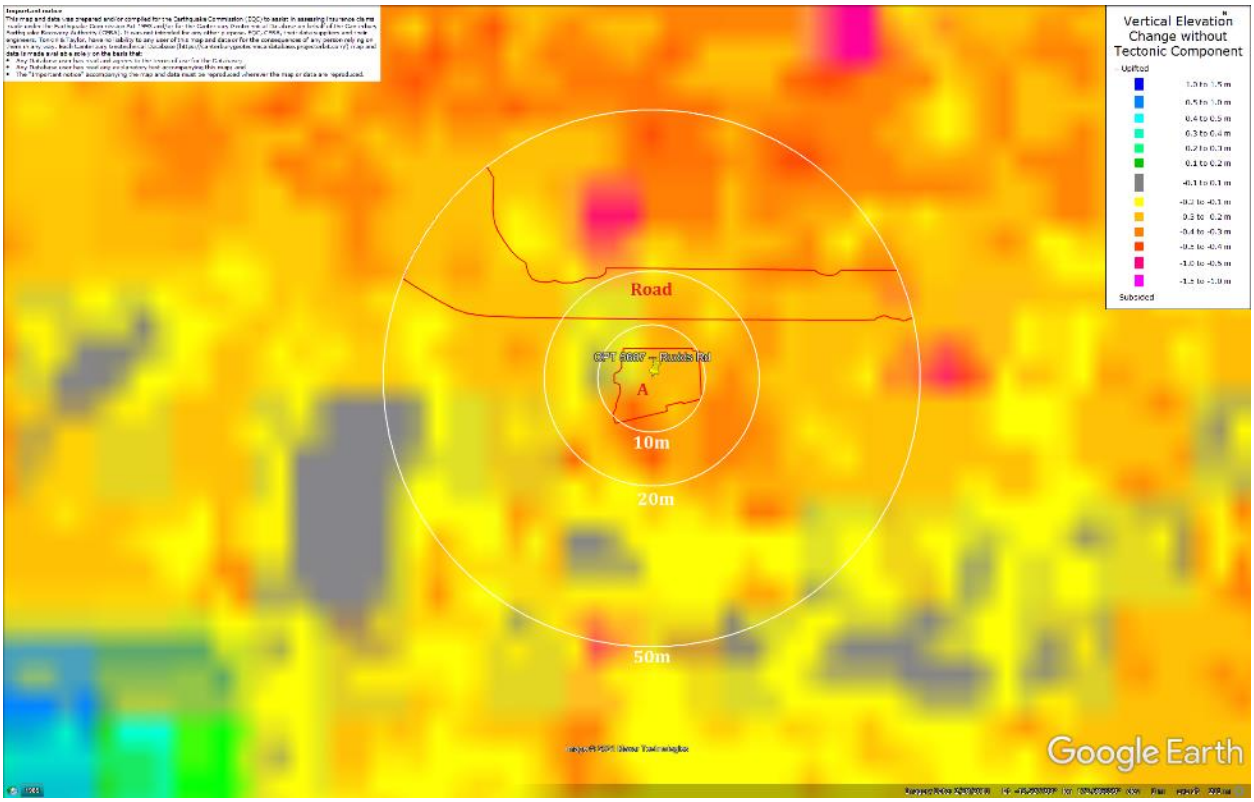

Figure 36: Ground surface subsidence without tectonic component for Feb 2011 Earthquake according to the LiDAR DEM.

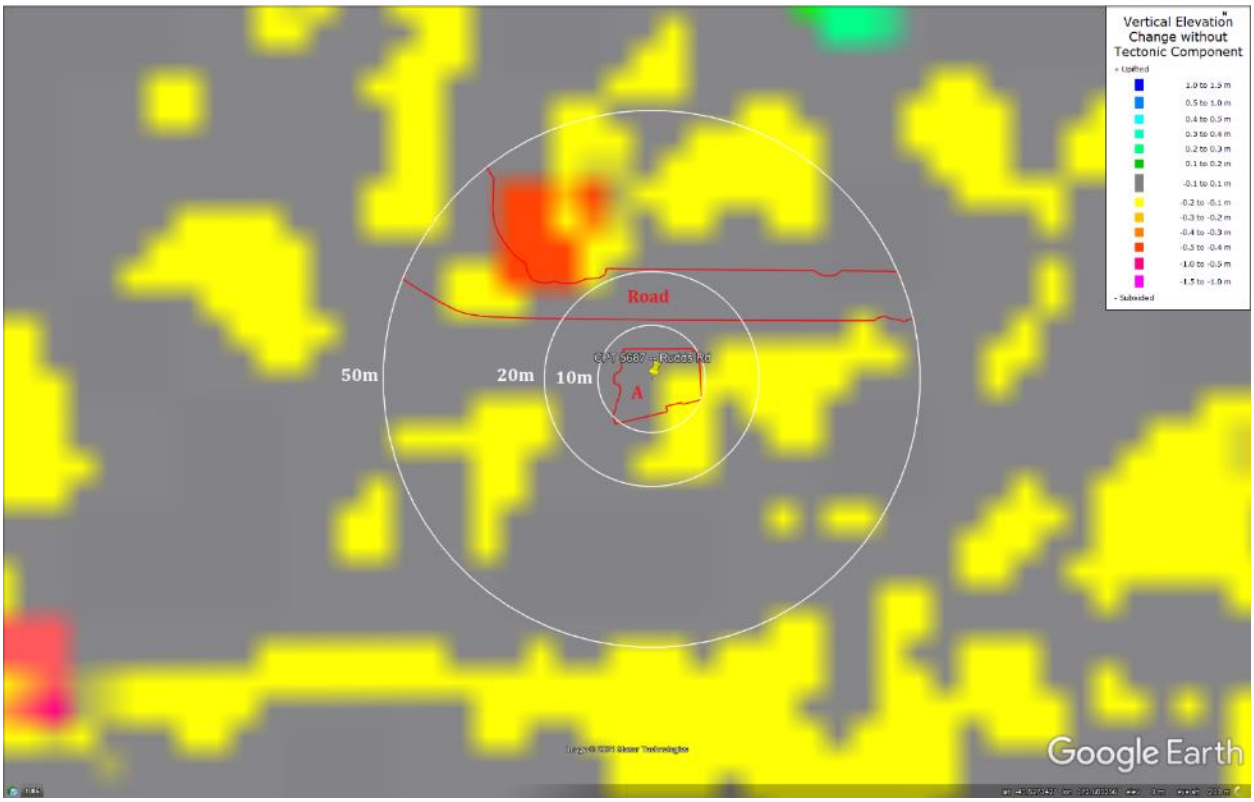

Figure 37: Ground surface subsidence without tectonic component for June 2011 Earthquake according to the LiDAR DEM.

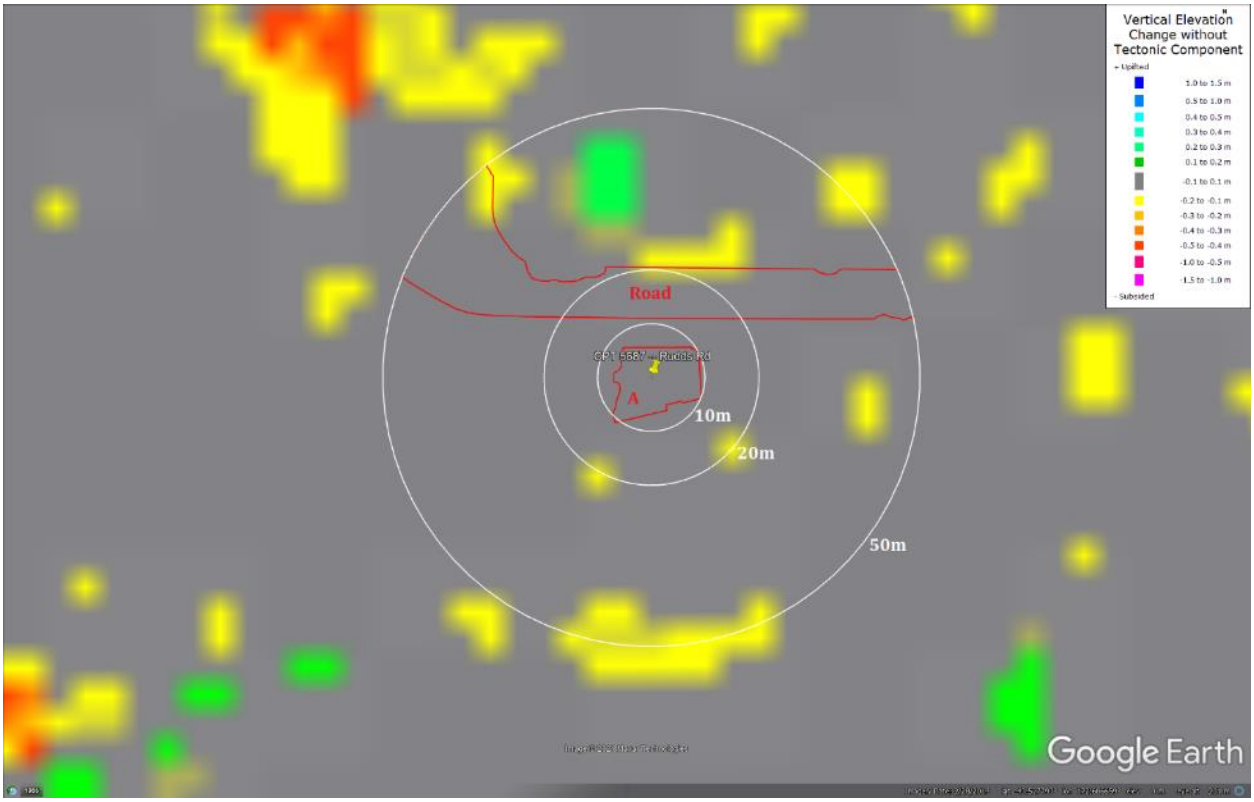

Figure 38: Ground surface subsidence without tectonic component for Dec 2011 Earthquake according to the LiDAR DEM.

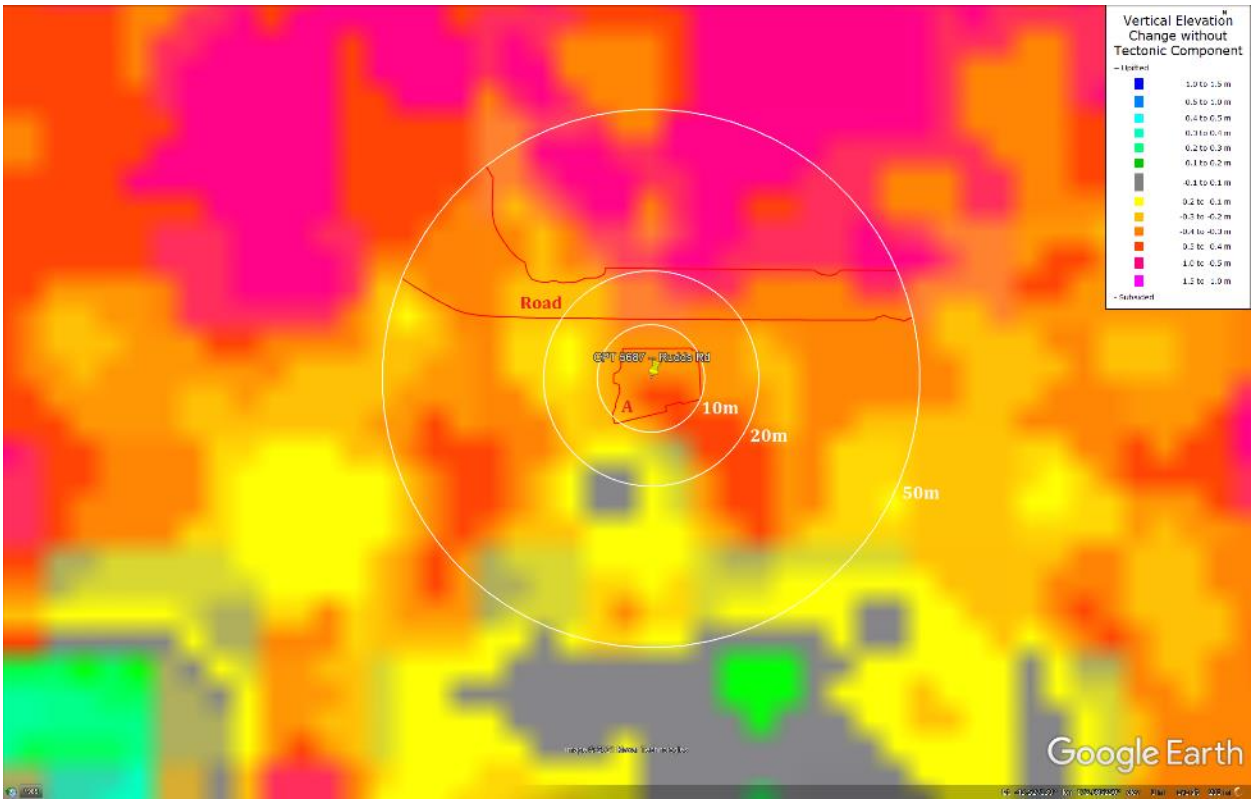

Figure 39: Ground surface subsidence without tectonic component for Canterbury Earthquake Sequence according to the LiDAR DEM.

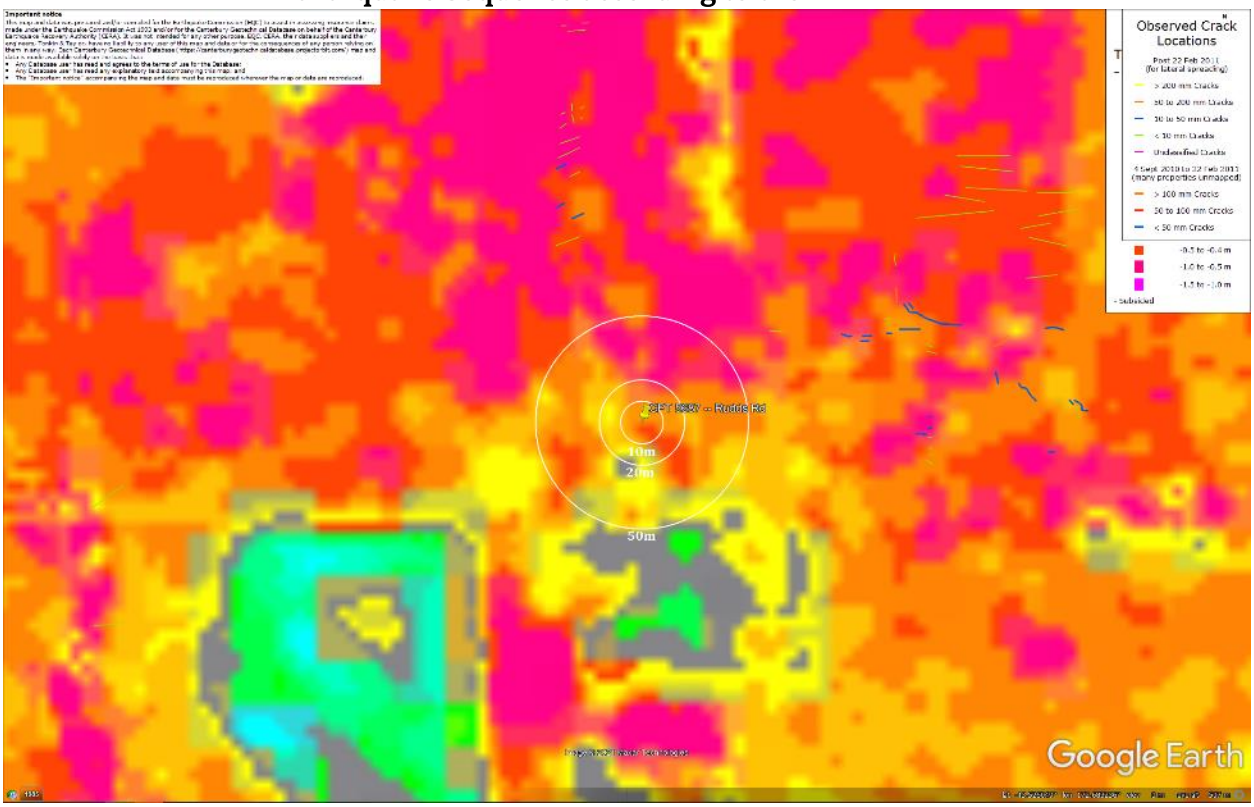

Figure 40: No lateral spreading for Canterbury Earthquake Sequence.

Figure 41: Vertical tectonic movements for Sep 2010 Earthquake.

Figure 42: Vertical tectonic movements for Feb 2011 Earthquake.

Figure 43: Vertical tectonic movements for June 2011 Earthquake.

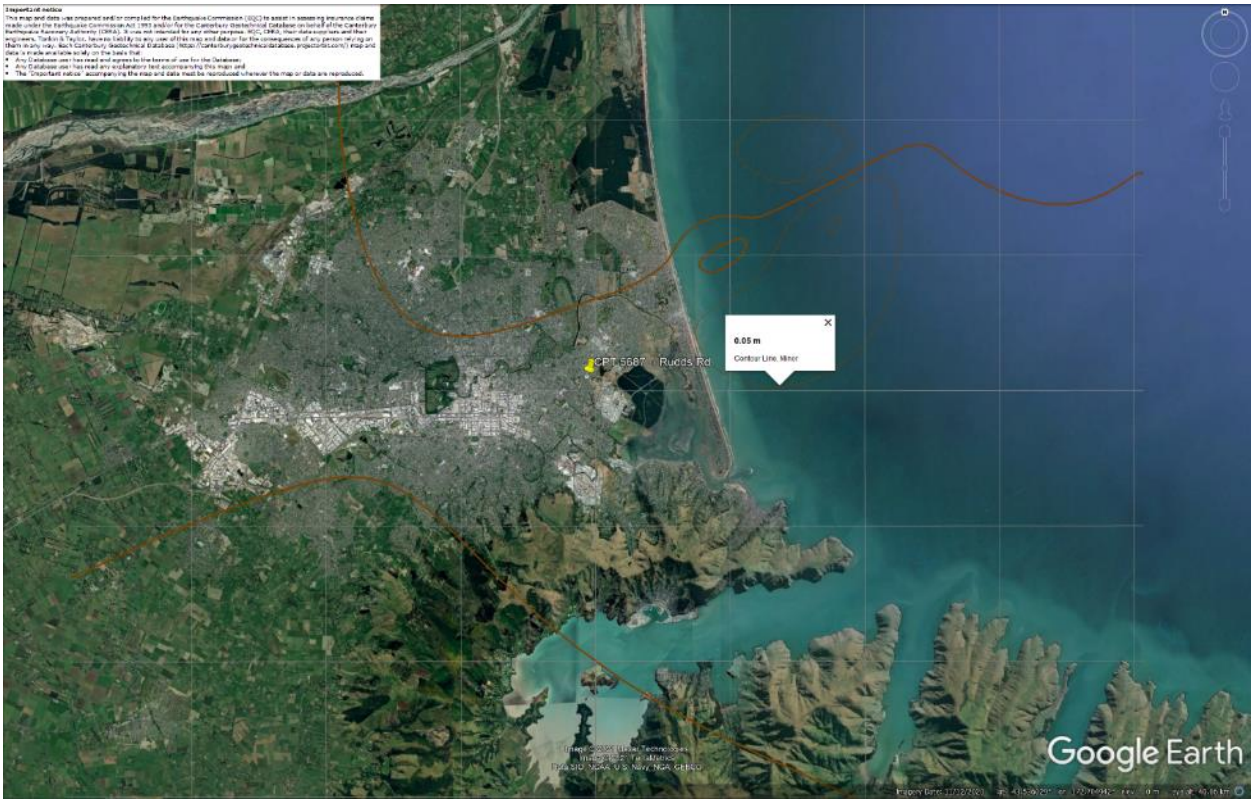

Figure 44: Vertical tectonic movements for Dec 2011 Earthquake.

Figure 45: Vertical tectonic movements for Canterbury Earthquake Sequence.

Figure 46: Aerial photograph showing the ejecta outline at the site for Feb-11 EQ.

Figure 47: Aerial photograph acquired on 16 Jun 2011 showing the ejecta outline at the site for Jun-11 EQ.

Figure 48: LDAT inspection notes for the property with Patch A (date: Nov 2011).

Contents of this figure cannot be shared as doing so is restricted by a Non-Disclosure Agreement.

Figure 49: Ground photographs showing ejecta remnants within Patch A (photograph date: Nov 2011).

Figure 50: PGA for Sep-10 EQ (st. dev. = 0.225-0.250 ln units).

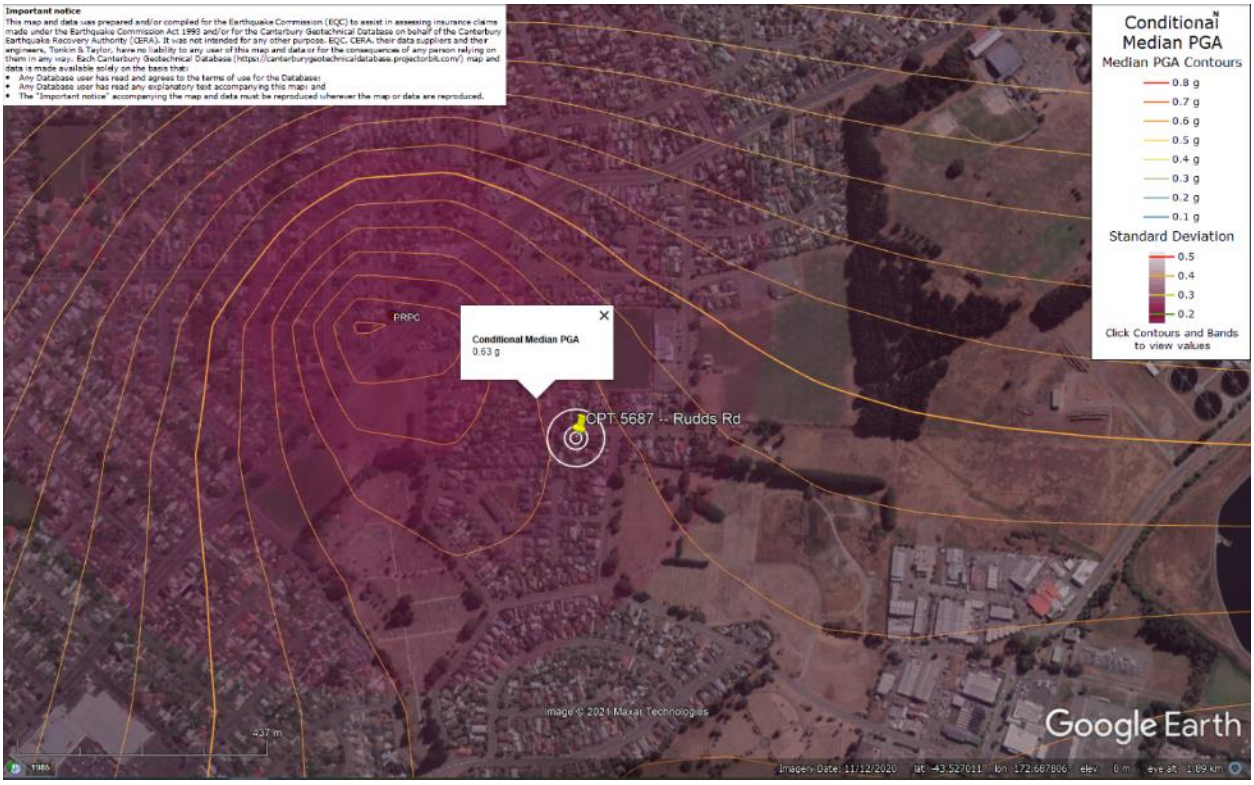

Figure 51: PGA for Feb-11 EQ (st. dev. = 0.250-0.275 ln units).

Figure 52: PGA for Jun-11 EQ (st. dev. = 0.250-0.275 ln units).

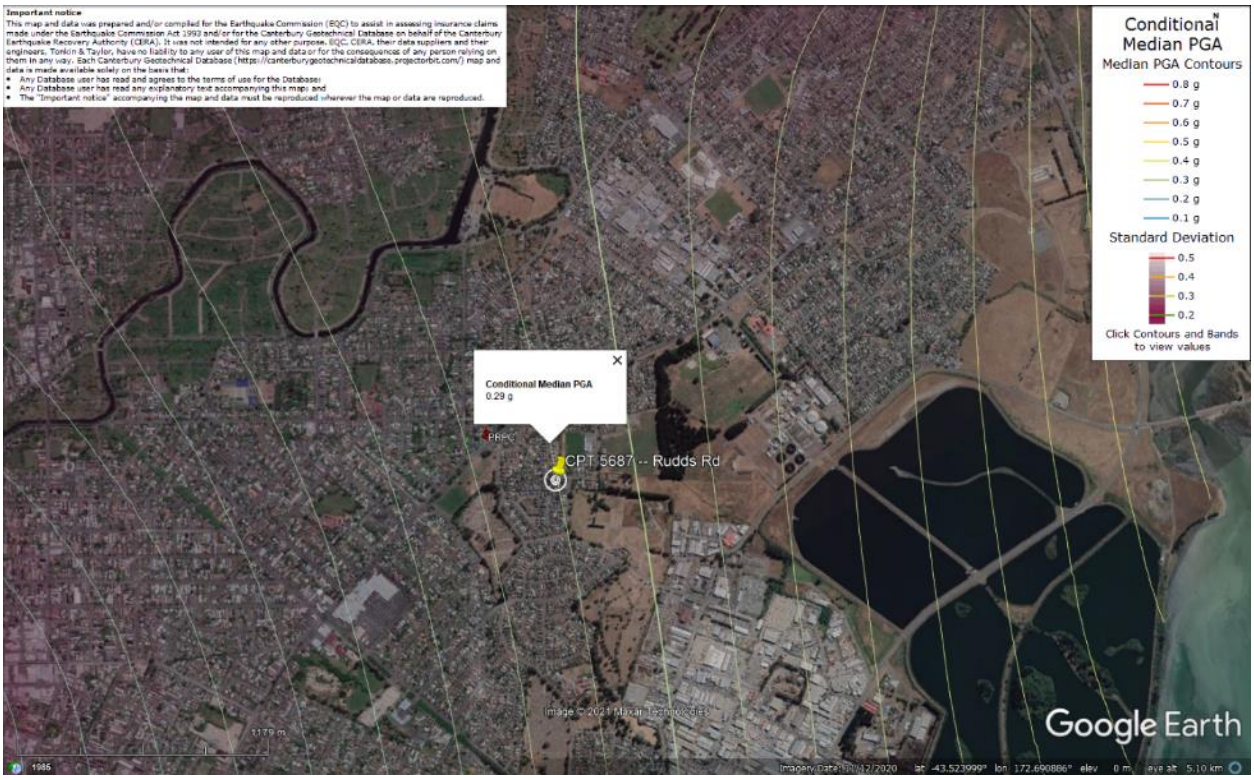

Figure 53: PGA for Dec-11 EQ (st. dev. = 0.400-0.425 ln units).

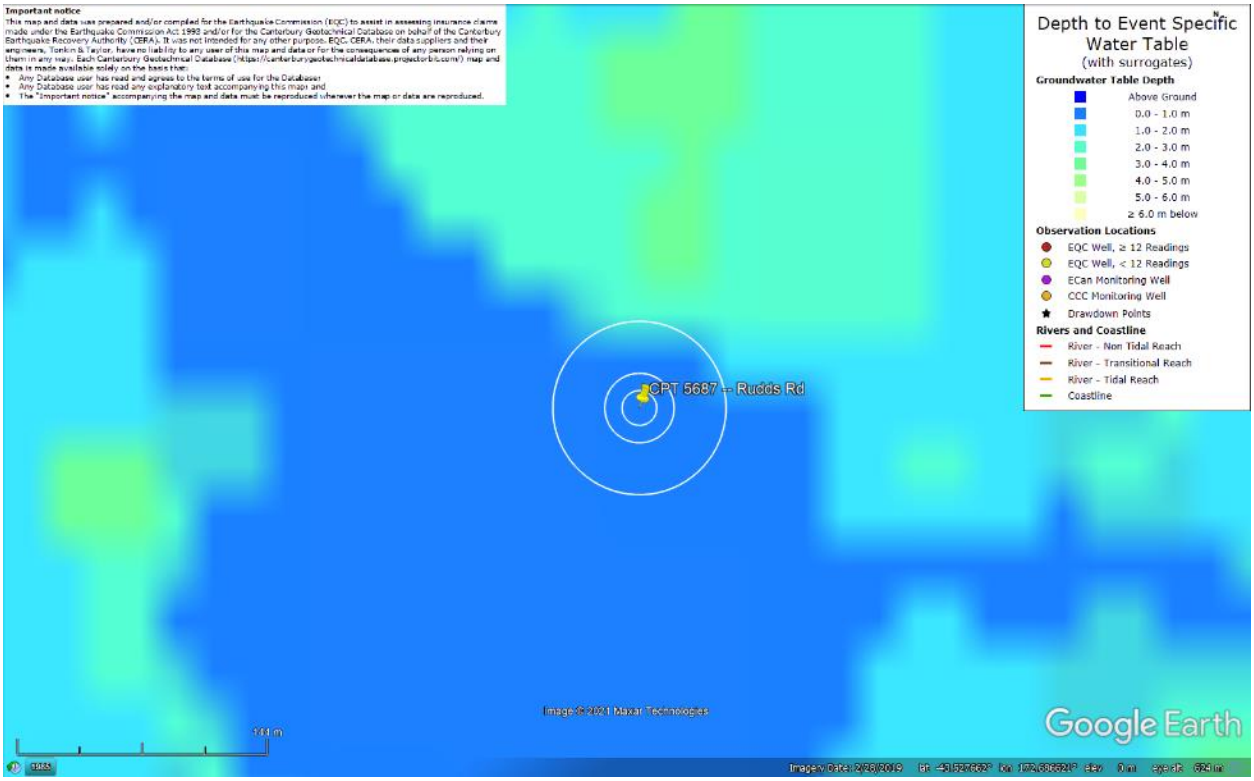

Figure 54: Depth to groundwater table for Sep-10 EQ.

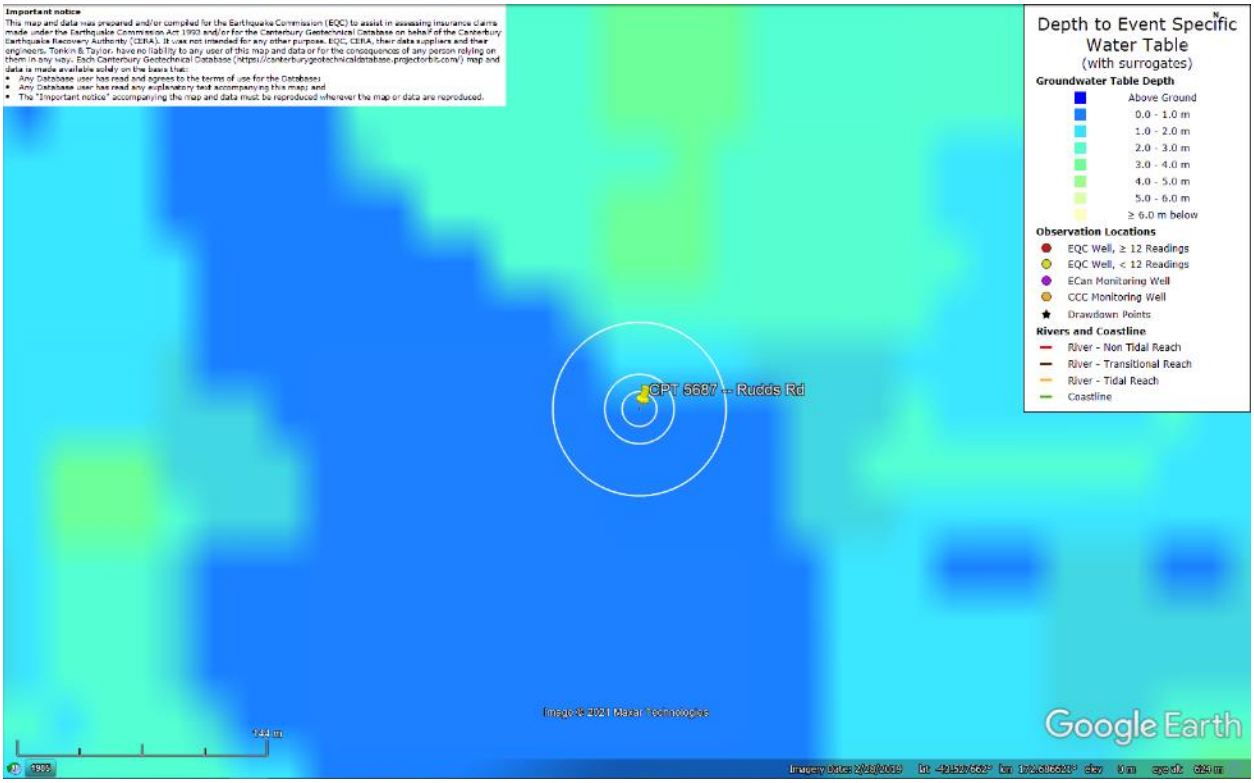

Figure 55: Depth to groundwater table for Feb-11 EQ.

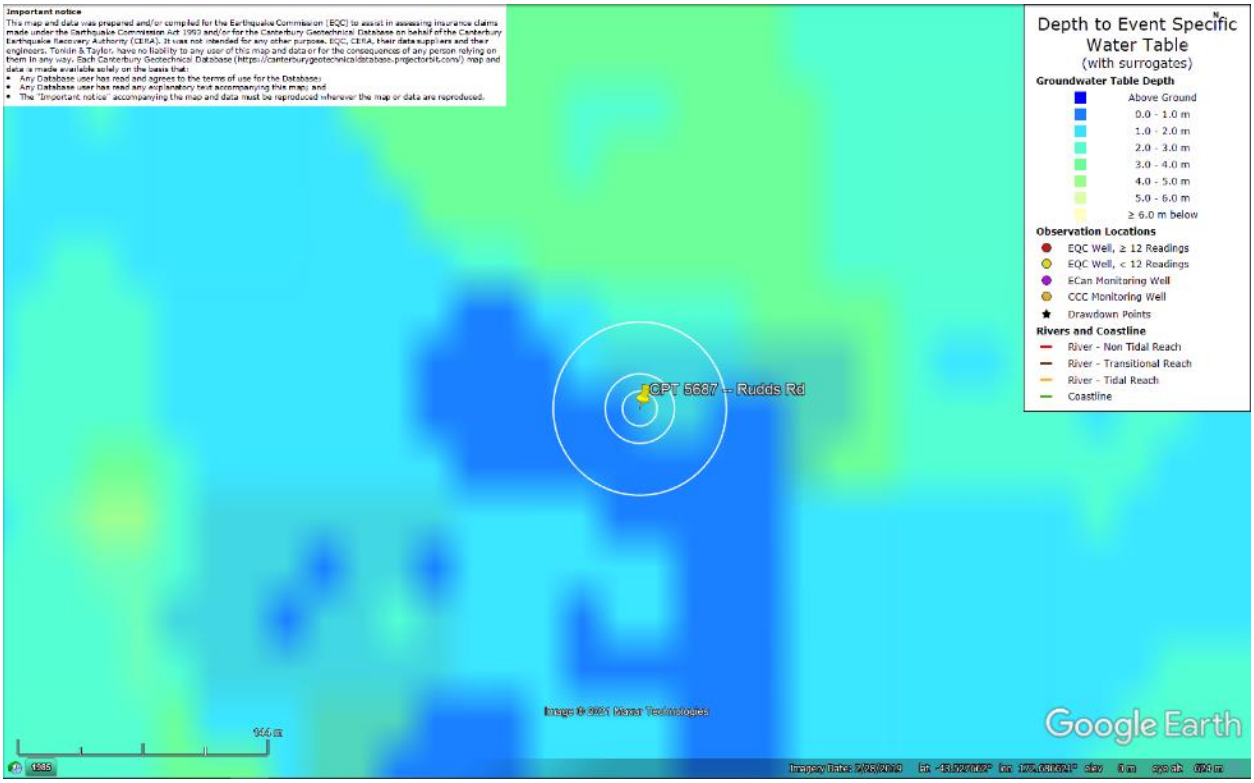

Figure 56: Depth to groundwater table for Jun-11 EQ.

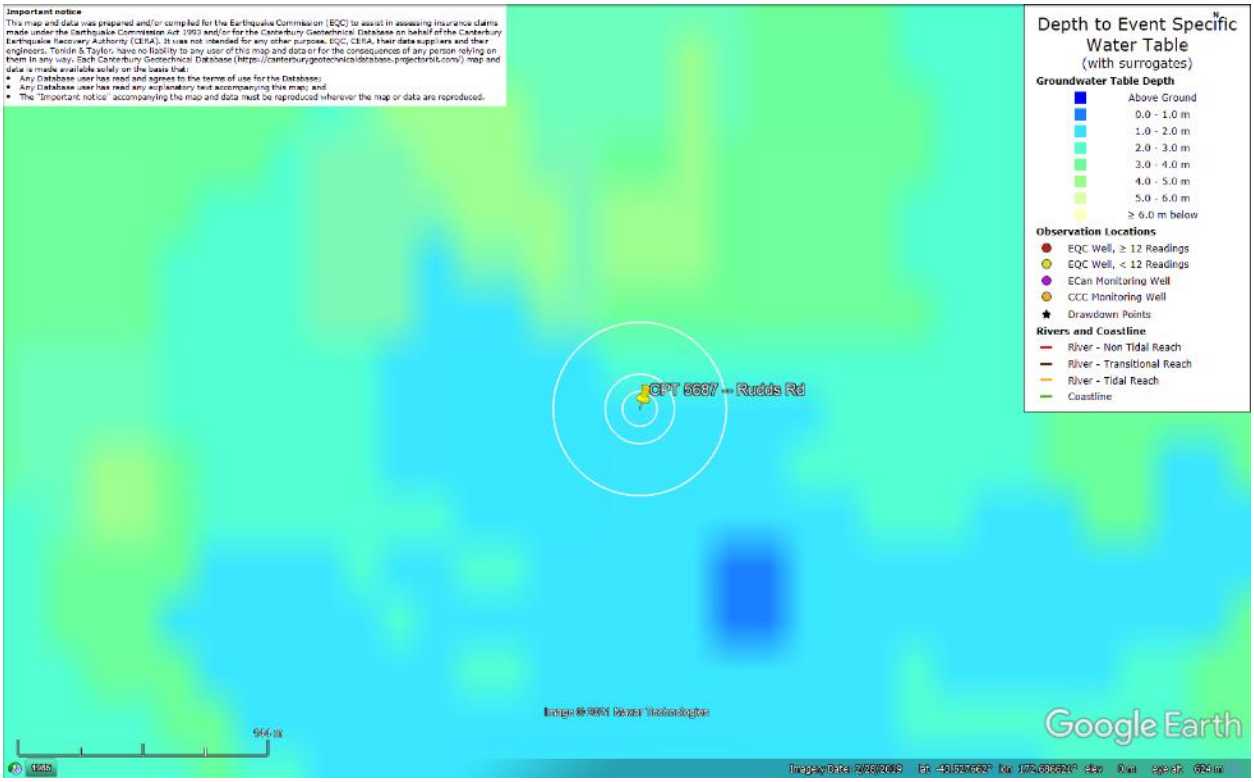

Figure 57: Depth to groundwater table for Dec-11 EQ.

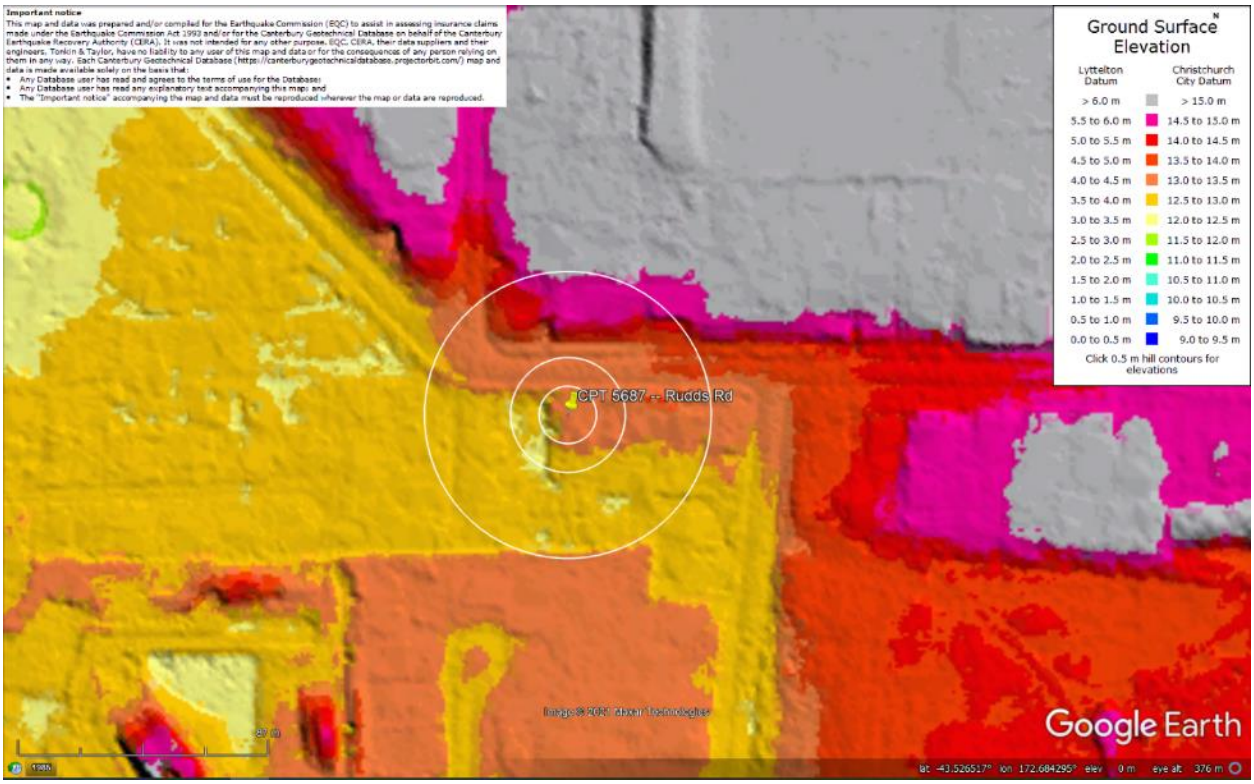

Figure 58: Ground surface elevation at the site according to the Sep-11 LiDAR survey.

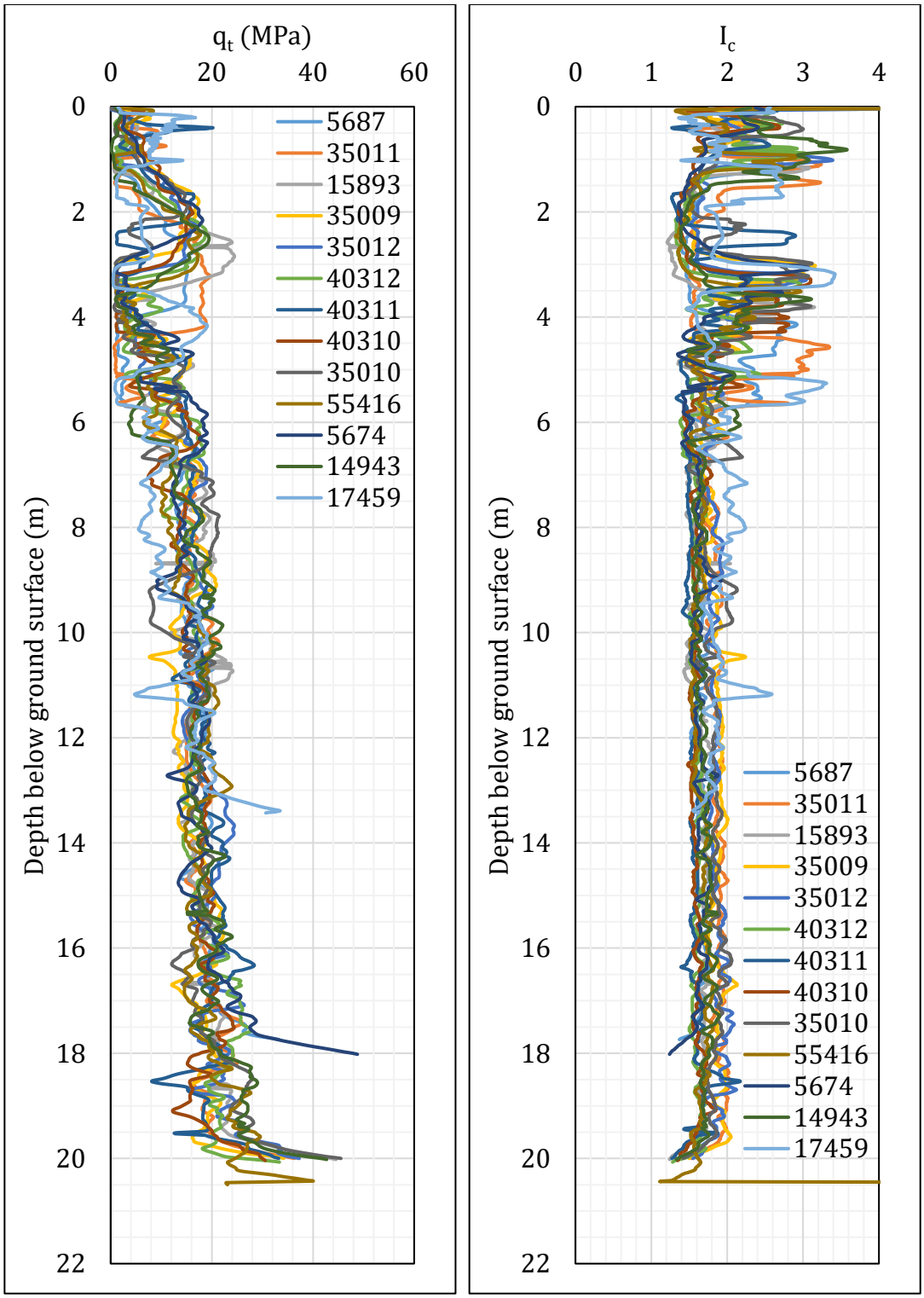

Figure 59: q_t and I_c profiles.

Note 5: The selection of CPTs for the area considered for settlement assessment (Figure 1) is based on the proximity of the CPTs to the considered areas. In accordance with that, the following table shows CPTs that were used for the volumetric settlement analysis in *Cliq v.3.0.3.2*, a CPT soil liquefaction software developed by GeoLogismiki. (The average volumetric settlements were reported in Table 8.)

Table 12: CPT profiles used in volumetric settlement analysis for areas selected for settlement assessment.

CPT ID No.	Patch A	Road (20-m buffer)	Road (50-m buffer)
5687	✓	✓	✓
35011	✓	✓	✓
15893		✓	✓
35009			
35012			
40312			✓
40311			
40310			
35010			
55416			
5674			
14943			✓
17459			✓

Note: CPTs 35011, 55416, and 14943 were used to compute the volumetric settlement for CPTs 5687 (17.74m-20m), 5674 (18.02m-20m), and 17459 (13.43m-20m), respectively.

Table 13a: CPT-based results.

EQ Event	Parameter	CPT ID 5687	35011	15893	35009	35012	40312	40311	$\Delta_{17.7m-20m}$
Sep-10	S_{V1D} (mm)	49	16	18	16	29	30	34	0
	LSN	18	3	7	4	7	12	13	0
	LPI	4	1	1	1	2	2	2	0
	LPI_{ish}	0	0	1	1	0	0	0	--
	$D_{FS<1}$ (m)	1.24	5.21	undet.	3.65	3.63	1	2.83	--
Feb-11	S_{V1D} (mm)	146	41	117	49	54	139	108	0
	LSN	38	12	26	13	17	30	33	0
	LPI	22	8	15	8	12	18	16	0
	LPI_{ish}	17	3	15	3	7	16	9	--
	$D_{FS<1}$ (m)	1.24	1.53	0.71	3.34	3.63	1	0.71	--
Jun-11	S_{V1D} (mm)	65	24	38	23	40	51	52	0
	LSN	21	5	8	6	10	15	17	0
	LPI	7	3	2	3	5	4	5	0
	LPI_{ish}	6	2	2	2	3	4	5	--
	$D_{FS<1}$ (m)	1.24	5.16	4.11	3.63	3.63	1.01	1.01	--
Dec-11	S_{V1D} (mm)	34	16	12	15	28	20	24	0
	LSN	7	3	3	4	7	4	7	0
	LPI	3	1	1	1	2	1	1	0
	LPI_{ish}	0	0	0	0	0	0	0	--
	$D_{FS<1}$ (m)	4.74	5.21	undet.	3.7	3.63	4.07	3.2	--

Notes: $D_{FS<1}$ = Depth to the first liquefiable layer ($FS_L<1$) that is at least 200-mm thick, as determined by the Boulanger and Idriss (2016) liquefaction-triggering procedure (P_L=50%, C_{FC}=0.13, and $I_{c,cutoff}$ =2.6), and exported from *Cliq v.3.0.3.2*; undet. = the specified soil layer was not detected; $\Delta_{17.7m-20m}$ indicates the amount of S_{V1D}, LSN, and LPI to be added to CPT 5687 due to its shallow penetration depth.

Table 13 (continued): CPT-based results.

EQ Event	Parameter	CPT ID 40310	35010	55416	5674	14943	17459	$\Delta_{18.0m-20m}$	$\Delta_{13.4m-20m}$
Sep-10	S_{V1D} (mm)	32	23	70	39	42	10	0	1
	LSN	7	6	21	12	12	2	0	0
	LPI	2	2	4	2	3	0	0	0
	LPI_{ish}	0	0	3	0	0	0	--	--
	$D_{FS<1}$ (m)	5.20	4.10	1.17	3.18	4.30	undet.	--	--
Feb-11	S_{V1D} (mm)	148	72	179	167	107	92	0	2
	LSN	27	24	40	35	25	19	0	0
	LPI	17	13	29	23	19	14	0	0
	LPI_{ish}	4	4	22	10	5	10	--	--
	$D_{FS<1}$ (m)	0.71	0.71	0.71	0.72	1.40	1.74	--	--
Jun-11	S_{V1D} (mm)	58	36	104	68	63	32	0	1
	LSN	9	9	25	14	17	5	0	0
	LPI	5	4	11	6	7	2	0	0
	LPI_{ish}	1	3	8	4	5	0	--	--
	$D_{FS<1}$ (m)	4.42	2.24	1.17	3.18	1.48	7.74	--	--
Dec-11	S_{V1D} (mm)	28	20	56	33	31	11	0	1
	LSN	5	5	11	8	7	2	0	0
	LPI	1	1	4	2	2	0	0	0
	LPI_{ish}	0	1	0	0	0	0	--	--
	$D_{FS<1}$ (m)	6.68	4.10	3.67	3.18	5.16	undet.	--	--

Notes: $D_{FS<1}$ = Depth to the first liquefiable layer ($FS_L<1$) that is at least 200-mm thick, as determined by the Boulanger and Idriss (2016) liquefaction-triggering procedure (P_L=50%, C_{FC}=0.13, and $I_{c,cutoff}$ =2.6), and exported from *Cliq v.3.0.3.2*; undet. = the specified soil layer was not detected; $\Delta_{18.0m-20m}$ and $\Delta_{13.4m-20m}$ indicate the amount of S_{V1D}, LSN, and LPI to be added to CPTs 5674 and 17459, respectively, due to their shallow penetration depths.

Note 6: Based on the borehole log (BH 16134, Figure 1), the groundwater table is at a depth of 1. 5 m below the ground surface. The soil profile consists of (1) fill of organic silt, OL, to a depth of 0.35 m, (2) fill consisting of silty sand, SM, to a depth of 1.0 m, (3) silty, ML, topsoil to a depth of 1.5 m, (4) fine to medium sand, SP, of the Christchurch formation to a depth of 4.4 m, (5) silty fine to medium sand, SM, of the Christchurch formation to a depth of 5.0 m, (6) silt, ML, of the Christchurch formation to a depth of 5.5 m, (7) silty fine to medium sand, SM, of the Christchurch formation to a depth of 6.1 m, (8) fine to medium sand, SP, of the Christchurch formation to a depth of 20 m.

Note 7: The ejecta-induced free-field settlement provided in Table 11 is an areal average settlement due to ejecta, which is based on the total settlement assessment area, A_T (provided in Table 9 and repeated in Table 14). However, the considered area was not always covered completely with ejecta; thus, it is important to provide the localized ejecta-induced settlement, too. The localized settlement due to ejecta is estimated using photographic evidence only as

$$S_{E,P\_localized} = \frac{V_E}{A_E}$$

where V_E is the total volume of ejecta within A_T and A_E is the total coverage area of ejecta within A_T. Please note that the areal ejecta-induced settlement provided in Table 14 as S_{E,P_areal} is the same as $S_{E,P}$ in Table 11, which was estimated as

$$S_{E,P\_areal} = S_{E,P} = \frac{V_E}{A_T}$$

where V_E is the total volume of ejecta within A_T and A_T is the total settlement assessment area.

Table 14a: Areal and localized ejecta-induced settlement estimates for Patch A (10-, 20-, and 50-m buffers) based on photographic evidence.

Earthquake Event	A_T (m^2)	A_E (m^2)	V_E (m^3)	S_{E,P_areal} (mm)	$S_{E,P\_localized}$ (mm)
Sep-10	168	0	0	0	0
Feb-11	160	96.4	4.3-7.2	35±10	60±15
Jun-11	164	41.9	1.5-2.6	15±5	50±15
Dec-11	168	0	0	0	0

Notes: S_{E,P_areal} = $S_{E,P}$ reported in Table 11 = areal ejecta-induced settlement; $S_{E,P\_localized}$ = localized ejecta-induced settlement; A_T = total settlement assessment area; V_E = total volume of ejecta within A_T; A_E = total area of ejecta within A_T; The estimates of both areal and localized ejecta-induced settlement are rounded to the nearest 5; Final plus/minus values are also rounded to the nearest 5.

Table 14b: Areal and localized ejecta-induced settlement estimates for Road (20-m buffer) based on photographic evidence.

Earthquake Event	A_T (m^2)	A_E (m^2)	V_E (m^3)	S_{E,P_areal} (mm)	$S_{E,P\_localized}$ (mm)
Sep-10	226	0	0	0	0
Feb-11	226	17.3	0.04-0.07	<5	5±5
Jun-11	210	99.7	0.2-0.4	<5	5±5
Dec-11	226	0	0	0	0

Notes: S_{E,P_areal} = $S_{E,P}$ reported in Table 11 = areal ejecta-induced settlement; $S_{E,P\_localized}$ = localized ejecta-induced settlement; A_T = total settlement assessment area; V_E = total volume of ejecta within A_T; A_E = total area of ejecta within A_T; The estimates of both areal and localized ejecta-induced settlement are rounded to the nearest 5; Final plus/minus values are also rounded to the nearest 5.

Table 14c: Areal and localized ejecta-induced settlement estimates for Road (50-m buffer) based on photographic evidence.

Earthquake Event	A_T (m^2)	A_E (m^2)	V_E (m^3)	S_{E,P_areal} (mm)	$S_{E,P\_localized}$ (mm)
Sep-10	1052	0	0	0	0
Feb-11	1052	97.5	0.4-0.8	<5	5±5
Jun-11	952	270	0.5-1.1	<5	5±5
Dec-11	1052	0	0	0	0

Notes: S_{E,P_areal} = $S_{E,P}$ reported in Table 11 = areal ejecta-induced settlement; $S_{E,P\_localized}$ = localized ejecta-induced settlement; A_T = total settlement assessment area; V_E = total volume of ejecta within A_T; A_E = total area of ejecta within A_T; The estimates of both areal and localized ejecta-induced settlement are rounded to the nearest 5; Final plus/minus values are also rounded to the nearest 5.

Summary 2:

- **The best estimate of the localized ejecta-induced free-field ground settlement at the Rudds Rd site for the SEP 2010, FEB 2011, JUN 2011, and DEC 2011 earthquake is 0 mm, 60±15 mm, 50±15 mm, and 0 mm, respectively.**
- **The best estimate of the localized ejecta-induced free-field settlement of the road at the Rudds Rd site for the SEP 2010, FEB 2011, JUN 2011, and DEC 2011 earthquake is 0 mm, 5±5 mm, 5±5 mm, and 0 mm, respectively.**